LABORATORY INVESTIGATION OF ELECTRICAL DISSIPATION OF WARM FOG

Leslie Bruce Herman

NAVAL POSTGRADUATE SCHOOL
Monterey, California

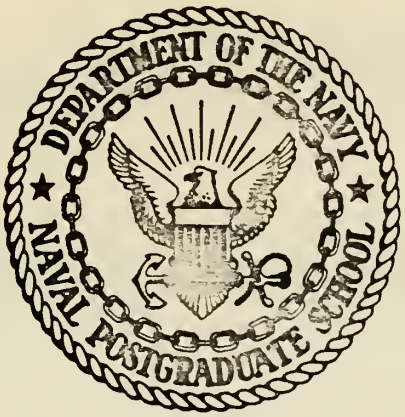

THESIS

LABORATORY INVESTIGATION OF ELECTRICAL DISSIPATION OF WARM FOG

by

Leslie Bruce Herman

Thesis Advisor: G. E. Schacher

December 1973

Approved for public release; distribution unlimited.

Laboratory Investigation of Electrical Dissipation of Warm Fog

by

Leslie Bruce Herman
Captain, United States Marine Corps
B.S., United States Naval Academy, 1965

Submitted in partial fulfillment of the
requirements for the degree of

MASTER OF SCIENCE IN PHYSICS

from the

NAVAL POSTGRADUATE SCHOOL
December 1973

ABSTRACT

A 27-cubic-foot fog chamber was constructed to investigate fog clearing by electrical means. Fogging of the chamber was accomplished with a spray nozzle driven by pre-humidified air, producing water droplets ranging from 10μ to 75μ. A corona discharge head in the center of the chamber was operated from 0 to 100 kV and measurements of fog conditions were made optically and with coated slides placed at various positions in the chamber. Rapid clearing was caused by the corona discharge. The dominant clearing mechanisms identified were coalescence and pushing of charged droplets to the walls of the chamber; the small size of the chamber precluded determination of which mechanism would be most important in large-scale fog clearing.

TABLE OF CONTENTS

LIST OF TABLES

LIST OF FIGURES

I. INTRODUCTION

As modern technology progresses the old cliche "everyone talks about the weather but no one does anything about it" is becoming more and more of a falsehood. The emphasis placed on environmental problems has led to a considerable expenditure of effort on many phases of weather modification. One of the areas that has received a concentrated effort is the dispersal of warm fog.

Fog is a common phenomenon in nature, but the theory of fog development and its dispersal is still in its infancy. At our present state of knowledge we have a lack of basic understanding to enable knowledgeable treatment of practical applications of fog modification. Fog is classified as either warm fog or supercooled fog, depending on the ambient temperature of the medium. Dissipation of supercooled fog (below 0° C) has achieved considerable success with a variety of methods; however, warm fog is more persistant and more insidious. Presently, no practical method has been devised to enable the dissipation of warm fog, though there has been considerable expenditure of money and effort on its investigation.

Fog, in either case, consists of a visible aggregate of minute water droplets suspended in air. Its formation by homogeneous vapor condensation is possible only in an atmosphere of supersaturated vapor. According to international

definition, fog reduces the visibility to less than one kilometer (Huschke, 1959); this is the criterion that distinguishes fog from haze and mist.

Fog, in lowering the visibility in the atmosphere, interferes with normal flight schedules, ship timetables, trains, automobile and military operations. The average individual usually has experienced one or more of these types of inconveniences. Not only is the individual hampered by fog but it also results in increased travel costs; for example, it is estimated that the U. S. airline industry loses more than 75 million dollars annually due to airport shutdowns involving fog (Gourdine, July 1972). Fog has been a contributing factor in numerous aircraft accidents and major highway accidents. In view of these facts the airline industry and the government have allocated large amounts of money for methods to combat fog.

The United States military is deeply involved in all aspects of weather modification. It has devoted considerable attention to fog dispersal because of the fact that so much of our defense is predicated on air power. If the armed forces are unable to utilize all their resources in combating a foe, they have failed in their calling. Naval aviators who hold Standard Instrument Cards are authorized to take off when the weather is 300-foot ceiling and one-mile visibility (OPNAV INST. 3710.1F). All naval aviators of single-piloted aircraft are authorized to land with a 200-foot ceiling and 1/2-mile visibility (OPNAV INST. 3710.1F). Once fog is

present the visibility, by definition, is less than take-off minimums and close to landing minimums. We, therefore, have greatly reduced the safe operation of one of the major weapons of the armed forces. It is because of this and the great loss of money to the commercial aviation industry that the development of ecologically safe fog dispersal systems is being investigated primarily for aviation requirements.

II. NATURE OF THE PROBLEM

A. DROPLET GROWTH

Water droplets can grow in one of two ways: (1) diffusion of water vapor and (2) collision (assuming coalescence) with other droplets. Growth by diffusion occurs slowly because of the large number of droplets that are competing for the existing water vapor in an essentially equilibrium situation and natural collision as a growth mechanism is almost negligible. The two most prominant causes of collisions are random thermal agitation (Brownian Motion) and droplets of different terminal velocities interacting. Even if they interact, the collection efficiency of fog droplets is very low. Numerous investigators have shown that the collection efficiency is increased by the presence of an electric field and the presence of charge on the droplets (Pilié, 1966). These effects are reasonable and have been demonstrated in the laboratory.

B. PAST WORK

Both Arthur D. Little, Inc. (1956) and Plumlee (1964) have been able to demonstrate increased coalescence in the laboratory using electrical methods. Most of the other investigators (Houghton and Radford, 1938; Jiusto, 1964; Junge, 1958; and Pilié and Kochmond, 1967) feel that the theory of fog dispersal through electrical means is valid but it is not a practical approach to the problem. They have concluded that it is

impractical because the inherently small charge on natural fog droplets precludes the creation of an electric field sufficiently large to have an appreciable effect on coalescence on a large scale in the field.

An electrostatic field can act in several ways to disperse warm fog:

1. Electrostatic fields can cause the dissipation of fog by increasing the rate of collision of charged fog droplets onto land and water surfaces.

2. Electrostatic forces could cause the fog particles to move outward to drier regions of the atmosphere and evaporate (MacCready and Mee, 1965).

3. Fields can cause drops to collide due to dipolar attraction through the induced dipolar moments of the droplets.

Since the water molecule is dipolar in nature, the earth's electric field polarizes the droplets in a uniform manner. The droplets are positioned so that the unlike charges tend to overcome the aerodynamic force that reduces the collection efficiency. Calculations of the probability of coalescence of drops due to polarization forces have been made by Sartor (1960), Cohet (1951), Panthener (1947) and Shulepov and Dukhin (1962). It is felt that any additional electric field applied to natural fog would increase the number of droplets being polarized and thus increase the collection efficiency.

Houghton and Radford (1938) examined the Cottrell method of producing charged droplets of like sign by a corona

discharge. It was shown that a wire 50 m long at a height of 10 m and potential of six megavolts would produce a clearing rate of 200 m^3/sec within 10 m of the wire. Vounegut and Moore (1958) showed that it was possible to charge large quantities of Aitken nuclei with a corona discharge. The discharge was produced on a long wire stretched horizontally several meters above the ground. They used a 30 KVDC power supply on a seven km long .64 cm diameter wire and were able to measure the spray discharge as far as eight km downwind.

Arthur D. Little, Inc. (1956) reported that the precipitation and coalescence of warm fog particles were enhanced by the application of an electric field. When the test was moved to the field no conclusive results could be shown. It has been stated that if the tests were run on a larger scale or under more favorable conditions the results could have been more conclusive (MacCready and Mee, 1965).

Since the aircraft industry is deeply involved in the investigation, the use of fixed-wing aircraft generating corona discharge has been examined. MacCready and Mee (1965) proposed the idea that corona current being discharged from the opposite wingtips of a flying aircraft would enhance fog dispersal. The method would discharge positive polarity from one wingtip and negative polarity from the other using the wingtip vortices to mix the charges in the air. It was stated that approximately 3×10^5 electronic charges per cm^3 could be put into the wake. They calculated that this method would result in field strengths up to 300 V/cm until mixing;

then the fields would be neutralized through droplet coalescence. Junge (1958) proposed almost the same idea except that he required more than one aircraft. He theorized that two or more planes flying parallel courses, spraying out charge, could disperse the fog through electrostatic means. A variation on this technique would be the release of positive charges from an aircraft flying in the warm stratus and a towed vehicle below the stratus releasing opposite charge. This would result in the mixing of clear air with the fog and increase evaporation (MacCready and Mee, 1965).

An alternate approach to the corona discharge method was the use of alternating current corona discharge (Pilié, 1966). Pilié and Kochmond (1967) followed up this approach but found through calculation that the force of attraction between charged fog droplets was eight orders of magnitude less than the force of gravity.

Another school of thought approached the problem through the insertion of charged particles in the fog. Houghton and Radford (1938) reported that calculations showed that grains of sand 100μ diameter would have effective diameters of 380μ in sweeping out fog droplets if a maximum charge (Rayleigh Limit) was carried. The major problem would be the distribution of the grains of sand and the production of their charge. There would also be the problem of the sand when it settled on the earth. The idea of charged water droplets was investigated and it was found that their effective collision diameter

could be increased by a factor of 100 with the application of charge (Pauthenier, 1950).

The creation of downdrafts by ionic currents was attempted by Hagen (1961). An electric potential gradient was used on a vertical wire located in an inversion. The increased mixing was to have caused increased evaporation. Field testing was inconclusive.

The results of seeding laboratory fogs with triboelectric powders were reported by Lieberman (1960) without too much optimism. The only concrete outcome was that some fogs became more stable as a result of the seeding.

Gourdine Systems, Inc. (1971) developed a method where an electrical charge is imparted to a fog via direct energy conversion principle, or electrogasdynamics (EGD), so that the fog is electrically attracted to the ground. The electrogasdynamic spray gun used a supersonic jet of air to carry charged submicron water droplets deep into the fog where they would eventually mix with and attract fog droplets. Computations demonstrated that it would require 166 EGD guns to satisfactorily clean a 4000 x 50 x 30 meter volume of a stationary fog (Gourdine, 1971). For a fog drifting at 4 mph the number of guns to clear the same volume would increase to 3,320 (Gourdine, 1971). There have been no field tests at present but the number of guns required to clear an area seems inordinately high.

As is seen in the previous history of electrical methods of fog dispersal, there are many ideas but no definite

results. Laboratory investigations have been somewhat successful in application and there have been some inconclusive field tests. Human safety is of prime importance in the implementation of fog dispersal by electrical means. The lack of good solid data concerning the physical mechanism involved in fog dissipation and the power required to produce the modification is hindering the outcome of fog dispersal research. It has been shown that fog can be cleared on a small scale with the use of electricity but as to how, why and whether full-scale clearing can be successful, the questions remain unanswered.

C. OBJECTIVE

Since fog dispersal by electrical methods is in its infancy, the object of this research is to identify and clarify the physical mechanism responsible for electric dissipation of fog. The initial idea was to construct a small fog chamber, conduct optical measurements during electrical dispersion, then expand the experiment to the field. The optical measurements showed that the rate of clearing increased with applied voltage but no conclusions could be reached concerning the phenomena responsible for the clearing. At this point it was decided to continue laboratory studies with experiments designed to allow determination of the dominant mechanism connected with the observed clearing. Since the use of coated slides is a recognized technique in meteorological research it was felt that their employment

would aid in our understanding. Several experiments, that are described in detail in what follows, were performed and coupled with the optical measurements, allowed several mechanisms to be identified: pushing, coalescence and droplet charging. These mechanisms are the phenomena that have to be understood to enable practical employment of electrical methods of warm fog dispersal.

III. EQUIPMENT

A. GENERAL

An overall schematic of the experimental equipment is shown in Figure 1. The central component is the fog chamber itself, which has three groups of associated equipment: (1) optical apparatus, (2) high voltage system, and (3) fog production apparatus.

The optical apparatus consists of a light source which shines into the chamber from the outside and is controlled by a variac so the light level can be adjusted. Scattered light intensity is measured with a photometer using a photomultiplier. The photometer output is displayed on a strip chart recorder so that continuous intensity measurements can be made.

High voltage is supplied by a sealed transformer/rectifier tank which utilizes 60 Hz voltage input. Output voltage is controlled by a variac on the input voltage. The input current is monitored as a check for leakage current, which can indicate faulty operation of the equipment. The output voltage is monitored using special terminals supplied on the tank, not directly on the high voltage output.

The fog is produced using an atomizer spray nozzle. Distilled water is supplied to the nozzle from a tank with a level control so that a constant water head is maintained at all times. The air used in the atomizer passes through

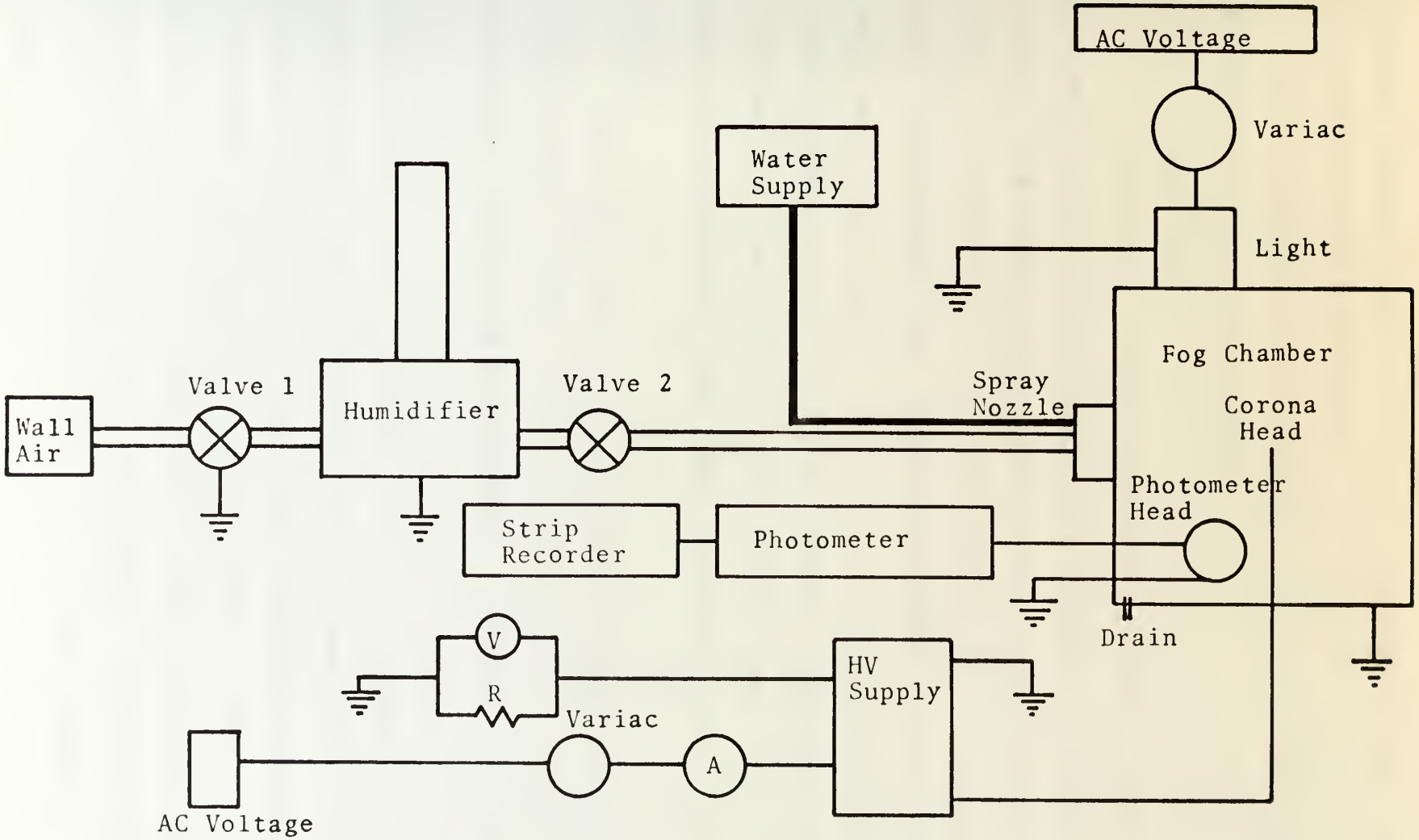

Figure 1. Schematic diagram of experimental equipment.

a humidifier so that use of the fog supply will not change the humidity in the chamber.

The various pieces of equipment and their operation are described in more detail below.

1. Fog Chamber

Initially, a frame made from 2 x 4 inch lumber was covered on four sides with 3/4-inch plywood. The front and rear of this chamber were covered with 1/4-inch thick plexiglass. The plywood on top of the box was fixed in place with four 5/16-inch bolts and removable allowing access to the interior of the chamber. A 1/2 x 1/4-inch foam strip was placed around the top lip of the chamber, forming a seal with the top plywood cover. The outside dimensions of the chamber are 30 inches wide, 30 inches high, and 36 inches long.

The first optical measurements attempted were transmitted light intensity through the fog, using a light source behind the chamber and a photometer in front. The front-rear plexiglass windows were abandoned when it was found that accurate optical readings could not be taken with this configuration. The photometer would become overloaded as the fog cleared and the data became meaningless even though a workable fog was present in the chamber. Thus, the rear of the chamber was covered with 1/4-inch plywood and the plexiglass and light source were moved to the top of the chamber, the photometer remaining in front (Figure 2). This installation permitted the photometer to read light scattered

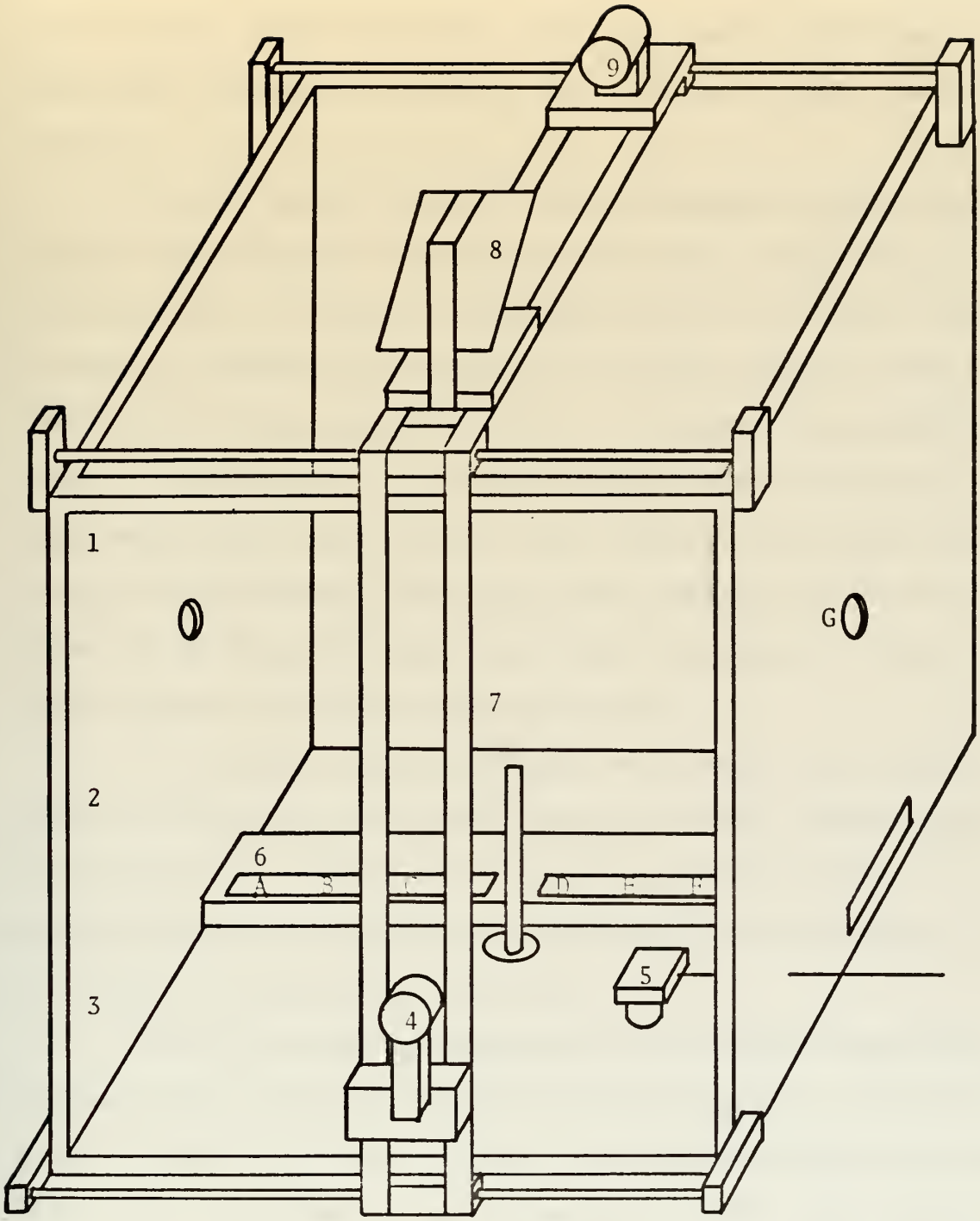

Figure 2. Fog chamber
1-3. Thermocouples
4. Photometer Head
5. Sloan Gauge
6. Plastic Slide Holder
7. Metal Frame
8. Mirror
9. Light
A-G. Slide Positions

at 90° by the water droplets. This technique permitted meaningful readings throughout the duration of fog in the chamber.

It was found that the front plexiglass window would collect water droplets through an inherent static charge on the window (a dramatic demonstration of this effect could be seen by rubbing the window and watching droplets form immediately on the region rubbed). To correct this deficiency the front plexiglass window was replaced with a 1/8-inch thick sheet of window glass. This construction permitted good optical readings since the glass remained relatively clear during fog generation, and could be heated if any water droplets did collect on the glass.

The interior of the chamber was coated with three quarts of Envirotex, a plastic paint used for waterproofing. This coating was rather shiny and hampered the optical measurements due to internal reflections, so the interior of the chamber was painted flat black.

With the chamber constructed as described above the fog duration inside was limited to approximately one minute. Blotter paper was added to the bottom of the chamber and the fog lasted approximately two minutes with this modification. Thus, the entire interior of the chamber was covered with blotter paper and saturated with distilled water maintaining the humidity in the chamber as close to saturation as possible. With this modification on the morning after a previous day's fog run, a very light fog was often observed to form in the

chamber while the front glass was being heated prior to optical measurements.

To prepare the chamber and equipment for the application of high voltage to the charging electrode, copper screening and grounding cables were attached to the chamber's interior, with the exception of the viewing windows. The screen was then covered with blotter paper. The copper screen was connected to ground with a grounding strap. These safety precautions also obviated the problem of residual charge remaining in the chamber.

Several access holes were cut into the chamber to allow insertion of various equipments. A 1-1/4-inch diameter hole was cut in the left side of the chamber for the fog input. A 2-1/2-inch diameter hole was cut in the center of the bottom of the chamber, which served a dual purpose: it allowed slides to be exposed and it permitted insertion of the high voltage cable with supporting structure. A 1-1/2-inch by five-inch access slot was cut into the right side of the chamber allowing insertion of a plastic slide holder. The slot was located in the center of the slide and next to the base of the chamber. A 1-1/4-inch hole was cut in the center of the right side of the chamber directly opposite the corona discharge head. The hole was used initially with a mass analyzer and later it afforded access for slides. A final hole was cut in the bottom of the chamber, eight inches from the right side and eight inches from the front. This 1-1/4-inch hole was fitted with a

foam rubber internal sheath and a foam rubber shutter covering the hole. This hole was used with the mass analyzer. All holes were sealed with stoppers when not in use.

Due to the large amount of water entering the chamber as fog a drain was placed in the rear corner. A 1/2-inch diameter Tygon tubing was inserted at this point to carry water into a container placed below the chamber. When the chamber was operating approximately two litre/hr of water was collected.

2. Fog Generation

a. Steam

Initially, steam was considered as a primary source of fog. The initial generator was mounted on the side of the chamber and heated electrically. Only a small amount of steam was produced so Marchetti's (1972) method was tried using identical equipment but it was found that the differential temperature between the steam and the plexiglass caused sufficient condensation to form to make the viewing window opaque. After several attempts at clearing, steam was abandoned as a fog medium.

b. Atomizer

(1) Room Air. An all-glass atomizer was constructed to produce an aerosol for fog generation. Compressed air from the building outlet was used to run the generator, the pressure ranging between 10-25 psi. The atomizer was contained in a large 10-inch diameter globe to collect large droplets, carrying them back to the water supply. A hole

in the side of the globe allowed the smaller droplets (10μ - 25μ) to escape into the fog chamber. The duration of the fog produced was approximately one minute. Readings taken of fog duration over a period of several days showed a correlation between outside temperature and the lifetime of the fog. The relative humidity of the compressed air being used to run the generator was checked and found to be between 30% to 50%. The air flowing into the chamber was so dry that it caused rapid evaporation of the fog.

(2) Humidified Air. A packed column (Figure 3) was designed to increase the humidity of the compressed air. Distilled water was pumped to the top of a column of ceramic beads and allowed to flow through the beads to a reservoir at the bottom. A water pump driven by an electric motor maintained circulation. The column was constructed from aluminum and contained six litres of water in the reservoir. Compressed air was fed into the top of the column adjacent to the water inlet and was drawn off at the bottom. Air that had been processed through the column showed a relative humidity between 85% and 98%, and generated a fog that would last in excess of 10 minutes. The use of humidified air was found to be the major advance in the operation of a fog chamber that would produce a sustained fog.

Even though the fog was of long duration, it was felt that a more dense fog was desired. A paint spray nozzle was tried in place of the glass atomizer, producing a longer lasting, more dense fog. Since the nozzle

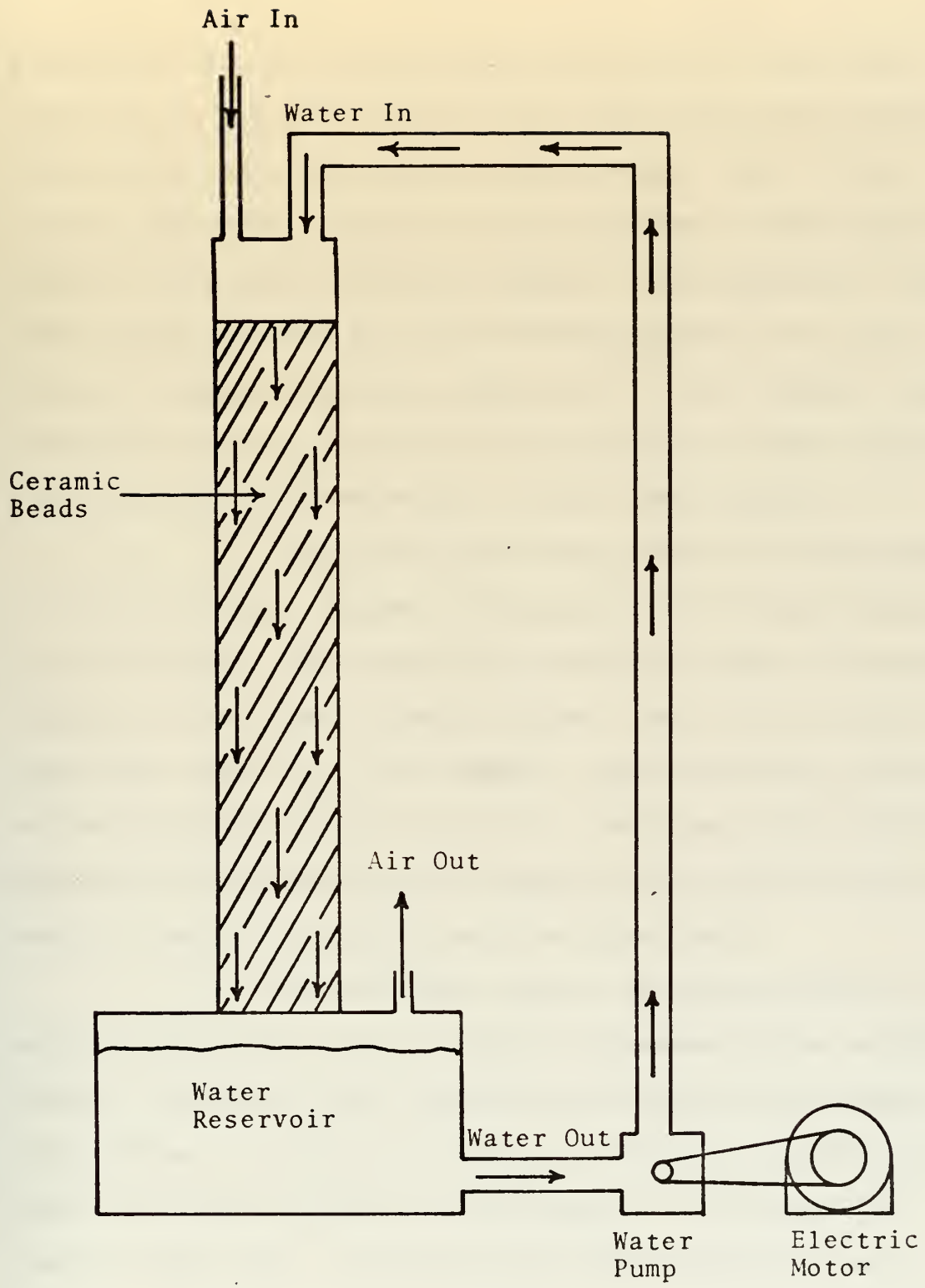

Figure 3. Packed column used to humidify air introduced into the fog chamber.

produced a droplet size distribution of 10μ - 75μ it was not necessary to utilize a system that separated large droplets (100μ) from the characteristic fog droplets (10μ - 50μ). The nozzle, therefore, supplied a great deal more water vapor per volume of air than the glass atomizer. Consequently, a more dense longer lasting fog was achieved because more water droplets per volume of air were injected into the chamber and it took more time for the natural processes (settling, evaporation and collision with the walls) to clear the chamber.

The spray nozzle was mounted on the center of the side of the chamber and angled at 70° toward the back of the chamber. This mounting reduced the amount of moisture splashed on the front viewing window. The initial spray head used water from a 3.5 litre beaker, which permitted one to two hours of continuous operation. The time of operation was dependent on the setting of a needle valve used to adjust the amount of water flowing through the spray head.

It was found that as the water level in the supply dropped the size of droplets produced by the nozzle varied. A constant head source was designed to alleviate this problem. A Fluidmaster Model 200 Ballcock toilet bowl check valve was mounted in the bottom of a 3-1/2-gallon plastic trash can. A plastic five-gallon water jug was mounted outside on the top of the copper cage, six feet above the trash can, to ensure enough water pressure to operate the check valve. The water bottle was connected to the check valve with 1/2-inch inside diameter Tygon tubing.

The water level in the trash can was maintained one inch above the top of the nozzle giving a positive water feed, a condition which produced the best fog. During operation it was noted that any small particles drawn into the spray nozzle would alter the spray. Thus a simple filter system was installed on the inlet to the spray nozzle.

A plastic spray head was constructed of the same dimensions as the metal one. It was run at 15 to 20 psi and produced a fog of the same duration and density. The reason for its construction was to test the effects of charging of the droplets by friction as they are produced. Since it was felt that any investigation into the charging of fog would be biased by this "picked up" charge it was decided to construct a nozzle from a non-conducting material. Later investigation showed that the material of the nozzle did not alter the charge on the droplets.

3. High Voltage Supply

The voltage was supplied by a Hipotronics HV DC supply number 26-334. The input to the supply was provided by a type W 20 HMT 3A Metered Variac Auto Transformer manufactured by General Radio Company. The variac permitted the output voltage to be varied from zero to 100 KVDC. The high voltage supply was located inside the copper screened cage next to the fog chamber while the variac was located outside the cage and could be controlled during operation.

A Digitec 262A multimeter was used to measure primary current in the HV tank. No attempt was made to

measure secondary current. Output voltage was measured with a Kiethly multimeter which was placed in parallel with a 400 K precision resistor across terminals provided on the HV tank. At 100 kV output voltage the terminal voltage was 100 volts with the 400 K ohm resistor in place.

The polarity of the charge being applied to the fog chamber could be selected by interchanging the ground and voltage leads at the HV tank. The voltage lead was placed in the chamber through the 2-1/2-inch diameter access hole in the bottom of the chamber. The corona discharge point was located in the geometrical center of the chamber and held in place with a 1/2-inch diameter teflon rod, mounted rigidly at the bottom of the chamber. To ensure a corona discharge by the high voltage cable three 1/2-inch long needles were inserted into the exposed end of the cable. It was felt that this would be sufficient to achieve the desired discharge.

4. Copper Cage

In the interest of the safety of the operator, all high voltage equipment was located inside a copper screened cage. The cage had a two-by-four framework which was covered with copper screening that was grounded. The dimensions of the cage are approximately eight feet on a side. The building wall formed two sides of the cage while a row of metal lockers formed the third side. The top and the front were covered with the copper screening. A door was located in the front as was a two foot by three foot plexiglass

viewing window. The placement of equipments with respect to the cage is as follows:

INTERIOR EQUIPMENT

1. Fog Chamber
2. HV DC Supply
3. Spray Head/Water Supply
4. Photometer
5. Light Source
6. Voltmeter
7. Chart Recorder

EXTERIOR EQUIPMENT

1. Five-Gallon Water Bottle
2. Ammeter
3. VARIAC for Light
4. VARIAC for HV Supply
5. Packed Column

All the equipment located inside the cage was grounded (Figure 1) as were the packed column and air shut-off valve located outside the cage. These precautions were necessary for safety during the operation of the HV supply and protection against residual static charge build-up on equipment as a result of the corona discharge.

B. MEASUREMENT

1. Slides

The coated slides were used to obtain both a size distribution and a droplet number distribution. These

measurements enabled a characterization of a standard, zero voltage fog, and allowed size and number comparisons when voltage was applied. Initially gelatin was tried as a slide coating but was rejected in favor of magnesium oxide. The bulk of the experimental data was obtained from slide measurements.

a. Gelatin

Initially standard glass specimen slides for microscope use were coated with a thin layer of gelatin. Even though the slides were precleaned, they were cleaned again with a 95% solution of ethyl alcohol, then allowed to dry in a relatively dust free atmosphere. This removed any packing residue that had coated the slides. To ensure relative purity, gelatin that was manufactured by Matheson, Coleman, and Bell, specified to be sufficient for culture media, was used. The gelatin was dissolved in warm distilled water in sufficient quantity to make a 2% solution. Schilling blue food coloring was added to the gelatin solution to increase the contrast of the slides. A clean glass rod was dipped into the colored gelatin solution and wiped once over the surface of the slide, giving a fairly uniform coating. The slides were dried in a draftless, dust free room for 24 hours. Once the slides were dry, they were stored in a standard bakelite tray.

It was found that slight unevenness of the gelatin coating forced a continual focusing of the microscope during droplet counting. This method was considered inadequate and different slide coatings were investigated.

b. Carbon Black

Another method is the coating of a standard cleaned slide with carbon black. Coating was accomplished with a small alcohol lamp filled with "nonflammable" cleaning solvent. The slide was passed through the flame until the carbon black built up to a sufficient thickness on the slide. The thickness of the coating was critical: If it were too thick, small droplets would not leave an impression. If it were too thin, the texture of the coating would mask the smaller droplets. Also, if the slide were allowed to get hot in the flame the carbon would burn into the glass and a permanent coating would be formed. When droplets impinged on these slides, they would leave a small black center surrounded by a white ring that was approximately the size of the droplet. This technique was not used because identical results had been obtained using magnesium smoke and greater expertise in the coating technique had been developed with that method.

c. Magnesium Oxide

Coating the slide with magnesium smoke is another recognized technique (May, 1945, 1950). Magnesium ribbon is burned and the smoke (MgO) is allowed to coat the slide. The application of the MgO and its limitations are identical to the carbon black technique. This is the coating used in the slide measurements reported here; it was the first method tried after the gelatin coating and desired results were achieved with a minimum of problems in coating technique.

2. Slide Holders

Since the use of slides was the major contribution to the data taken, several holders were designed and used. As it turned out, several holders were necessary at the same time to obtain the required information during a fog run.

a. Aluminum Holder

The first slide holder consisted of an aluminum flange that was fixed to the bottom of the chamber over the central access hole. A five-inch diameter 1-1/2-inch thick slide holder was machined from aluminum to fit into the flange. A 1-1/2-inch hole was partially bored in the center of the holder and fitted with an external valve to allow the slide holder to be attached to a weak vacuum line in order to draw very small droplets down to the slide. A three-inch diameter recess machined into the holder allowed the placement of slides and the use of a rubber O-ring for a seal. The holder design was such that only one slide at a time could be used and it had to be inserted and removed manually. Due to the manual manipulation necessary, this slide holder could not be used during the application of high voltage, and it was not used for data reported here.

b. Plastic Holder

A plastic holder (Figure 4) was designed to allow the exposure of a strip of six slides. The holder was placed in the bottom center of the chamber allowing the slides to be positioned radially outward from the electrode (Figure 2).

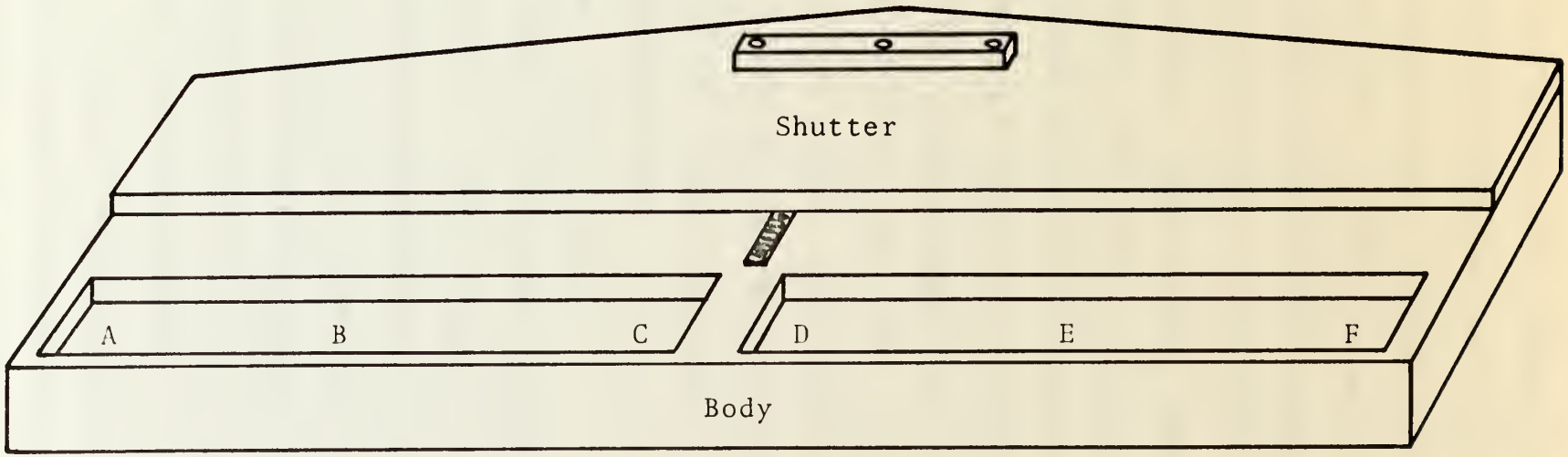

Figure 4. Plastic slide holder with slide positions A, B, C, D, E, and F listed. Shutter held in open position.

A recess was machined in the body of the holder so that three slides could be positioned either side of center; these positions were lettered A, B, C, D, E, F from left to right when viewed from the front of the chamber (Figure 2). A plastic shutter over the slides was held closed with a spring. A nylon string was attached to the shutter, passed through the rear of the chamber, over a pulley, and through the cage to the control desk. The holder was positioned through the access slot in the side of the chamber and held in position by the slot and a 1/4-inch bolt located opposite the slot. The bottom of the chamber, where the slide holder was to rest, was covered with a five-inch wide sheet of teflon to protect the blotter paper. This holder permitted the use of slides while voltage was being applied since it could be operated outside the cage. Operation of the shutter exposed all slides simultaneously.

c. Dual Shutter Holder

A third slide holder (Figure 5) was designed so a series of exposures could be taken in sections on a single slide. The initial design allowed only consecutive exposure of the sections without any time delay between the exposures. The holder was modified with a double shutter that permitted a time delay between exposures of the sections. The holder was constructed from a 3-1/2-inch by 3-1/2-inch by 1/4-inch plastic block. A recess was machined in the block to hold one slide and an attached aluminum strip positioned the holder in the chamber. Two independent shutters were used

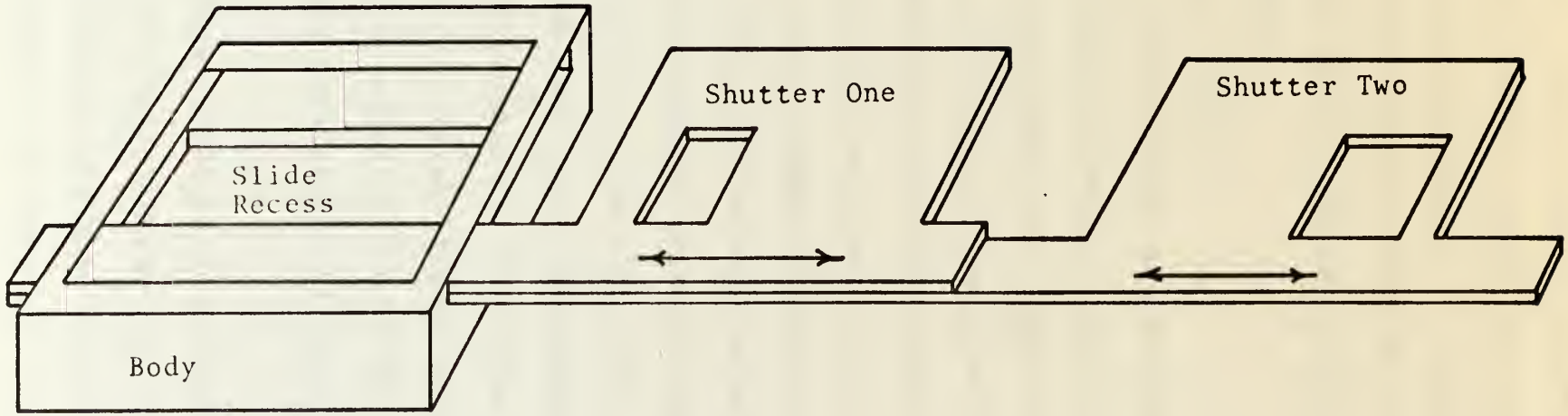

Figure 5. Dual-shutter slide holder with shutter removed from body for detailed viewing. Each shutter moves independently.

to expose the slides: one to select the portion of the slide to be exposed and the other to expose the slide to the fog. This slide holder was positioned in the chamber through the side access hole. Once the holder was in position, the access hole was sealed with a styrofoam plug to ensure the integrity of the chamber.

d. Cardboard "Coffin"

A fourth slide holder was designed to take slides on the side of the chamber directly opposite the electrode. A cardboard "coffin" was made three inches long, one inch wide, 3/4 inch deep. The sides of this holder prevented droplets having predominantly downward motion from striking the slide. The holder was used when voltage was applied and gave an indication of any physical mechanism present in the chamber that would change the downward movement of the droplets. This holder was inserted into the chamber through the access hole at the center of the right-hand side. A piece of heavy cloth hung on the side of the chamber directly over the holder acted as a shutter for the slide. Gravity held the shutter closed and a string leading out of the box allowed the cloth to be raised, exposing the slide. This holder could be operated during the application of high voltage.

3. Microscope

The slides were inspected on a Bausch and Lomb Model 52 Dynazoom Bench Metallograph Microscope using ten power magnification. Two scales were used while viewing: One was a scale that allowed size measurement; the other was a

10 x 10 grid used for counting. A Polaroid camera back was an integral part of the microscope and allowed pictures to be taken of various slides. An external light source was used to provide illumination of the slides. The microscope has a 2X zoom feature but most of the observations were in the 1X mode.

4. Optical Measurements

To simplify optical measurements a frame was constructed to allow the mounting of the photocell and the light source to the same rigid structure, keeping source-detector geometry constant. The frame was constructed of aluminum angle stock (Figure 2). Two strips of angle were attached 4-1/2 inches apart to make a track for the photocell mount, and for the light. The light and photocell tracks were welded together, forming a 90° angle between them. At the ends of the photocell track and the light source track, roller bearings were fitted and the entire unit moved on two tracks of 1/2-inch diameter stainless steel rod attached to the chamber, one at the bottom of the front face and the other at the rear of the top. The entire frame could be moved left and right, while the light moved fore and aft over the top window and the photocell up and down facing the front window. The front face of the chamber was quartered and numbered, starting at the top left quarter, clockwise 1, 2, 3, 4. The photocell was positioned in the geometric center of each of the four sections when optical measurements were performed.

Optical readings from the fog were taken with a Gamma Scientific, Inc. Model 700 M log/linear photomultiplier photometer. A model 700-1 general purpose photomultiplier was mounted on the aluminum frame. Measurements were taken of the light scattered 90°. Thus, as the fog dissipated, the intensity of the scattered light decreased, and the photometer reading decreased.

Initially the high-intensity light source was mounted to shine directly through the top of the chamber. The intense heat from the bulb caused its early destruction. Therefore, the colimated light source was mounted in an upright position and the light beam directed down through the top of the chamber by a five-by-seven-inch plane mirror. The light was fixed in one position and the mirror was moved fore and aft to position the shaft of light in the chamber. The 120-volt, 200-watt GE CHK bulb still generated sufficient heat to necessitate the installation of a blower on the light housing, which cured the problem of the light burning out. The light source was connected to a type 116 Powerstat Variac that enabled the light intensity to be controlled in order to establish and control a repeatable baseline. The mirror was positioned so that the light shaft was located midway between the front and rear of the chamber for all of the measurements reported here.

The entire chamber was covered with a tent of blue cloth suspended from a 48-inch by 56-inch frame, suspended from the top of the copper cage with nylon twine. The blue

tent reduced external light, permitting readings to be taken with the room lights on. Background readings taken for various external light conditions showed no intensity variation in the interior of the chamber.

A model G-14 Varian Graphic Recorder was connected to the DC output of the photometer to take continuous scattered light readings. The photometer and strip recorder were located inside the copper cage. The scale of the photometer could be changed by a 1/2-inch diameter long plexiglass rod that attached to the scale switch and extended to the outside of the cage. The chart recorder could be started and stopped externally to the copper cage with a remote on/off plastic arm. All the equipment in the cage was grounded for safety. Remote non-conducting arms were used for safety because of the high DC voltages being utilized in the experiment.

5. Charge Measurements

Charge on the input fog droplets was measured using a one-inch diameter brass disc affixed to a plastic rod as the probe. The brass disc was inserted into the fog and current was measured with a Keithley 610 BR Electrometer. The measurements obtained allowed a calculation of the average charge on an average sized fog droplet entering the chamber. No measurements of charge were taken during the application of high voltage due to safety considerations.

6. Droplet Mass

An attempt was made to measure the density of the fog using a mass analyzer. A quartz crystal oscillating at

a certain resonant frequency will shift its frequency when it picks up mass. A sloan Thickness Gage based on this principle was used to examine the amount of fog incident on a quartz crystal surface. Due to problems with conduction between the contacts and crystal the investigation of the fog with this instrument had to be suspended. Use of this instrument could be very beneficial in the investigation of fogs if it could be made to operate satisfactorily.

7. Thermocouple

Temperature measurements were taken with three copper-constantan thermocouples inserted into the chamber at points 1, 2, and 3 (Figure 2). The purpose was to determine if there were temperature gradients in the chamber, which would lead to thermal mixing. The reference end of the thermocouple was attached to a solid copper slug 1-1/2 inches in diameter and six inches long. The reference was placed in an ice-water bath and allowed to stabilize for three hours prior to any measurements. A Kiethly 150 B Microvolt-Ammeter was used to measure thermocouple voltage. The selection of the particular temperature sensor being used was made with two knife switches so that only one point could be recorded at a time, but switching among the points was rapid. No temperature gradient was noted either with or without applied voltage between the three points chosen and no further investigation into thermal mixing was undertaken.

IV. EXPERIMENTAL TECHNIQUE AND RESULTS

Optical and slide measurements are the basis for the quantitative results reported here, but initial experimentation consisted of visual observations of the fog chamber under a variety of charging conditions. The rate of clearing that was observed was in direct relation to the strength of the voltage applied: the higher the voltage the more rapidly the chamber cleared.

The chamber was filled with fog and allowed to reach steady state before the fog generator was disconnected. Even though one could visually observe an increased clearing rate at voltages from 0 to 15 kV, the clearing was so gradual that the whole chamber appeared to clear uniformly. Around 30 kV it was obvious that the dissipation proceeded radially outward from the corona head to the walls of the chamber. When 50 kV was applied, a swirling, streaming action was observed radiating from the corona head and creating a rapidly expanding cleared spherical zone around the electrode. The amount of turbulence emanating from the corona head increased as the applied voltage increased up to the maximum of 100 kV. At this voltage the fog chamber would completely clear of fog in 10 to 15 seconds. The rate of clearing and the violence of the "pushing" of the fog prompted the making of a 16 mm movie to allow a more detailed visual study of the phenomena. The film confirms the visual observations and slow motion

sequences were especially dramatic, showing the turbulence and pushing action.

The initial sequence in the film shows the rapid fog production in the chamber with the metal nozzle. This sequence is followed by a 50 kV demonstration of fog dispersal which illustrates the swirling, streaming action of the corona. Several sequences were taken at reduced voltage for comparison and a sequence was made at 80 kV to dramatize the violent effect of fog clearing at high voltage. Copies of the film are available.

Fog clearing was attempted under continuous fog generation which resulted in some interesting observations. From 0 to 40 kV no clearing was observed but above 40 kV dissipation was evident. As the voltage was increased, the chamber became clearer until, at 80 kV, the only fog in the chamber was a stream about 10 inches long emanating from the nozzle. Above 80 kV the system shorted out and a fuse was blown in the ammeter. Between 40 and 80 kV it appeared that the fog was repelled by the corona and entering droplets were pushed away from the center of the chamber.

The original observations support the idea that the rate of fog dissipation is enhanced by injected charge. Once these qualitative measurements were completed, experiments were performed to identify the physical mechanisms responsible for the observed clearing. Because the pushing of the fog to the walls of the chamber is so rapid and violent at high voltage, it was felt that meaningful results could not be

obtained in that voltage regime. Thus, it was decided to perform the measurements from 0 to 15 kV.

The data section is divided into two separate areas: (1) optical measurements and (2) slide measurements. The slide measurements are also subdivided into three parts: (1) The first part is concerned with measurements taken without voltage application; (2) the second is concerned with measurements taken after a 15-second application of voltage, and (3) the final part is concerned with slides exposed during voltage application. The final averaged data tables are presented with the various plots of data.

A. OPTICAL MEASUREMENTS

Prior to any data being taken, the chamber had to be prefogged for two to three hours to ensure a relatively steady sate. The blotter paper was presoaked with water prior to the fogging to assure a relative humidity in the chamber that was as close to 100% as possible. Once the chamber had been sufficiently fogged, the front glass was heated slightly with a hot air blower to remove any condensation. This ensured a clear optical path through the glass and standardized the areas of measurement as far as the glass face was concerned. The blower was not run during the optical readings. Once the chamber was ready, the blue cloth was dropped and optical measurements could begin.

The light was positioned in the center of the top track and turned on at the beginning of the fogging to ensure

that the light would heat up and achieve steady state operation. The top plexiglass was cleaned on the outside to ensure a clear path into the interior of the chamber. The light was collimated to give a beam approximately three inches in diameter over its entire length.

The optical measurements were taken with the photometer head positioned on the rigid frame, geometrically centered in the particular quadrant of the front glass being used. The aperture on the photometer head was opened fully during measurements. Prior to each series of data the photometer was zeroed, with the aperture closed; then the strip chart recorder was zeroed. All equipment was turned on during the prefogging and left on during the entire run. The batteries in the photometer were checked daily and replaced when required. These precautions were necessary to ensure a repeatable baseline.

The scattered light background from the chamber was measured prior to prefogging and after the dissipation of the fog that was used for a run. The readings were different for each section on the front glass owing to variations in the chamber's interior; however, the background readings remained essentially the same for a particular section regardless of the day. The fog was considered dispersed when the optical reading approximately reached the background reading.

1. Zero Voltage

Once the chamber had been prefogged the first measurements of the series were taken without additional preparation. The strip recorder was started and the paper allowed to advance for 15 seconds. The fog was shut off at the valve when the recorder passed a t = 0 mark. The first measurements of each series were taken at zero voltage. The recorder was run until the reading stabilized near the background reading. Due to noise in the system there was some minor oscillation around the background reading.

2. Applied Voltage

Subsequent measurements were taken after the chamber was refogged for three minutes after the zero voltage measurement. During the fogging the photometer and strip recorder were rezeroed and the glass checked for condensation. After two minutes of refogging the optical reading would stabilize close to the value obtained during the first measurement. Once the reading was stabilized the light intensity was adjusted with the variac to ensure the same scattered light intensity starting point, ensuring a standard baseline. This technique was investigated and did not bias the measurements. The recorder was started and when the t = 0 mark was reached the fog was turned off and simultaneously the voltage was turned on; the voltage was left on until the fog was dissipated. The sequence of measurements followed for each section was 0 volts, 5 Kvolts, 10 Kvolts, 15 Kvolts.

Once measurements had been conducted in all four sections, the sequence was repeated four times for averaging purposes. A typical strip recording for 15 Kvolts is included in Figure 6 to demonstrate the method utilized for obtaining the data. Once the data were recorded from the strip chart, it was normalized to the intensity value at $t = 0$ for the particular voltage and panel. The normalized value was then averaged over the series of readings taken. The reduced normalized data are given in Table I.

Due to fluctuations of the recording caused by turbulence in the chamber and noise in the system, a smooth curve was drawn through the recorder readout, averaging the perturbations. This average value of the intensity was the data recorded and utilized in the computations of the normalized scattered intensity for the sequences measured. It is because of this averaging technique that an experimental error is assigned to each data point. The experimental error is ± 0.4 units on the normalized scale.

The scattered intensity is plotted versus time on a semi-log plot (Figure 7), for each section and for the various voltages used. The zero and 5 kV data do not show much increase in clearing in any of the four sections. A comparison of sections one and two with sections three and four in Figure 4 shows a longer lasting fog at zero and 5 kV for the latter two sections. This was expected since gravitational settling of the droplets maintained the fog's density in the lower regions of the chamber; the fog would clear

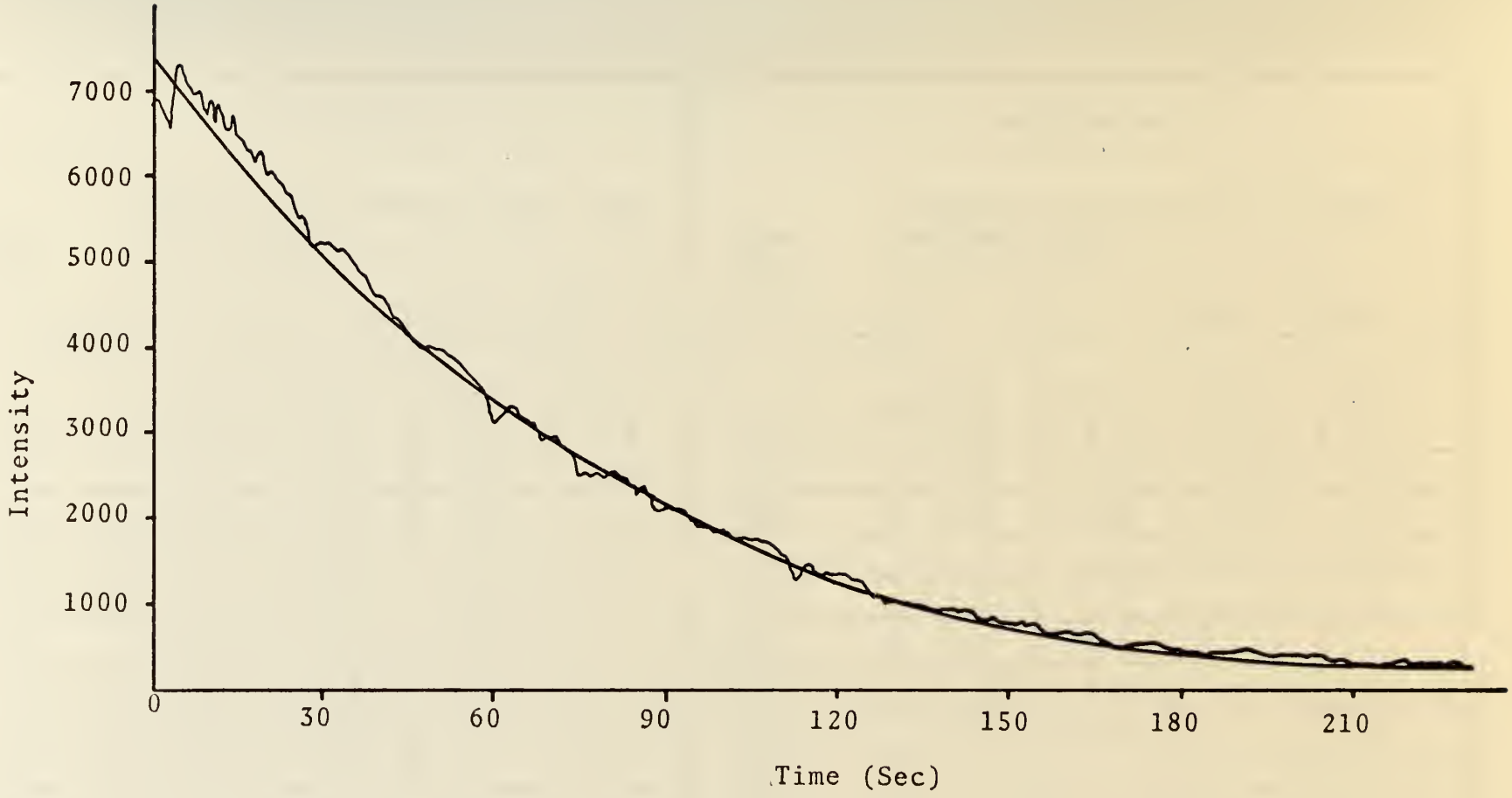

Figure 6. Sample optical data from strip recorder for 15 kV.

Section No. 1					Section No. 2				
Time (sec)	Normalized intensity for each voltage (kV)				Time (sec)	Normalized intensity for each voltage (kV)			
	0	5	10	15		0	5	10	15
0	10.0	10.0	10.0	10.0	0	10.0	10.0	10.0	10.0
30	8.8	9.0	8.0	5.9	30	9.0	8.9	8.2	5.3
60	6.6	6.5	4.5	2.6	60	6.5	6.2	5.0	2.4
90	4.5	4.4	3.0	1.1	90	4.5	4.3	2.6	0.8
120	3.2	3.3	1.7	0.6	120	3.3	2.8	1.5	0.3
150	2.1	2.4	1.2	0.3	150	2.1	2.0	1.0	--
180	1.4	1.6	0.9	--	180	1.5	1.6	--	--
210	0.8	0.8	0.5	--	210	1.2	1.0	--	--
240	0.5	0.6	--	--	240	0.5	0.4	--	--
270	0.4	0.4	--	--	270	--	--	--	--
300	--	--	--	--	300	--	--	--	--

Table I. Averaged normalized data for optical measurements at 0, 5, 10, and 15 kV as a function of time during voltage application.

(Table I continued on next page)

Section No. 3					Section No. 4				
Time (Sec)	Normalized intensity for each voltage (kV)				Time (Sec)	Normalized intensity for each voltage (kV)			
	0	5	10	15		0	5	10	15
0	10.0	10.0	10.0	10.0	0	10.0	10.0	10.0	10.0
30	9.6	9.3	8.1	6.0	30	9.0	9.0	8.2	5.0
60	7.4	7.3	5.7	3.0	60	7.0	7.0	5.6	2.4
90	5.7	5.7	3.9	1.4	90	5.2	5.2	3.5	1.1
120	4.6	4.6	2.7	--	120	4.3	4.3	2.2	0.5
150	3.7	4.0	2.0	--	150	3.6	3.6	1.7	--
180	3.3	3.6	--	--	180	3.1	3.0	--	--
210	2.4	3.0	--	--	210	2.5	2.6	--	--
240	2.0	2.5	--	--	240	2.3	2.1	--	--
270	1.5	--	--	--	270	2.0	1.8	--	--
300	--	--	--	--	300	1.7	--	--	--

Table I (continued). Averaged normalized data for optical measurements at 0, 5, 10, and 15 kV as a function of time during voltage application.

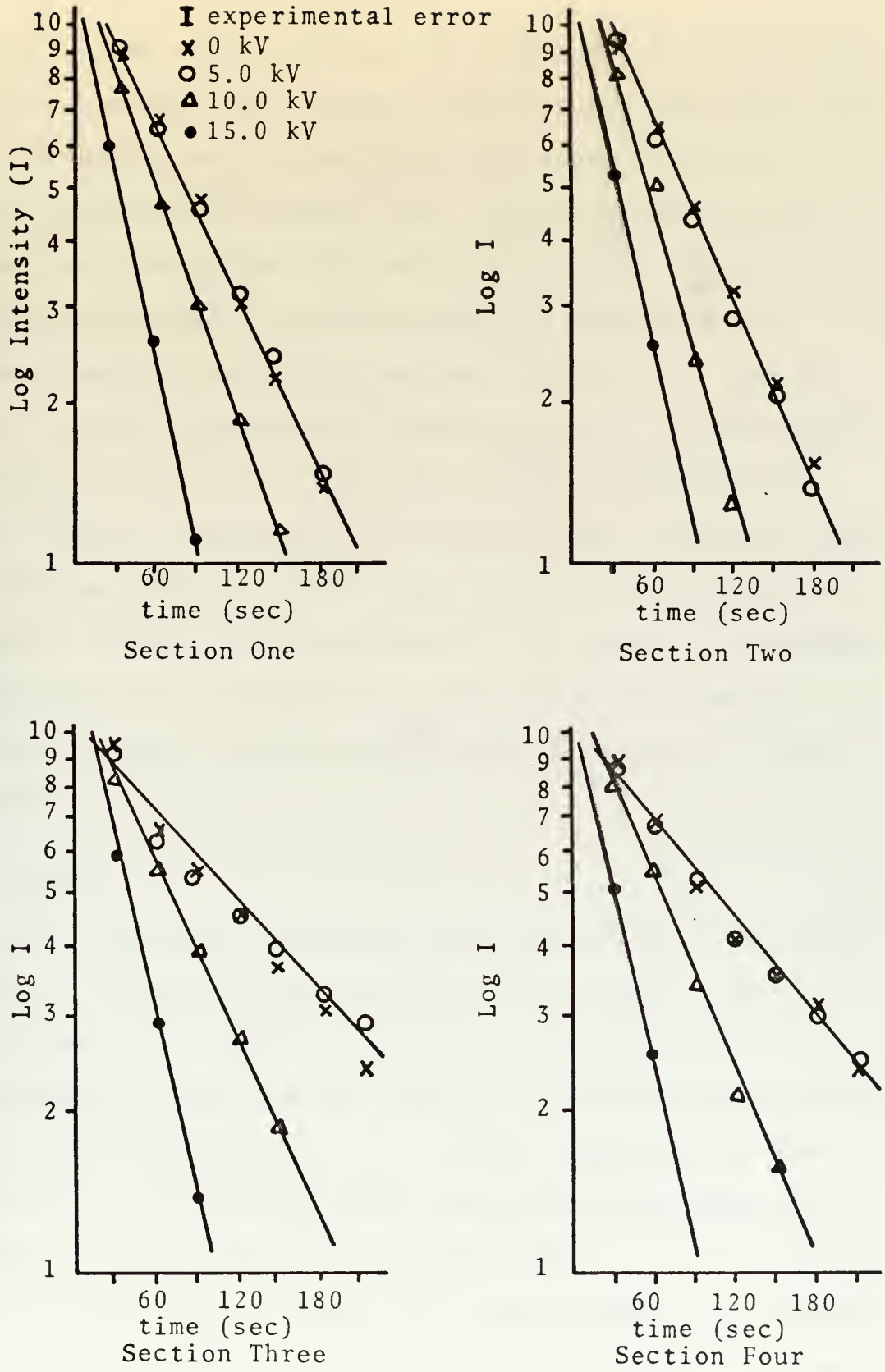

Figure 7. Averaged normalized optical intensity versus time for Sections 1 through 4 for voltages 0, 5, 10, and 15 kV.

naturally from top to bottom. At 10 kV and 15 kV data for all four sections were similar and reflected the effect of applied voltage on the previously explained settling. Visual observations did not show a clearing from top to bottom but from corona head radially outward. The time constants obtained from these plots are presented in Table II and plotted as VT_E versus V (Figure 8). The VT_E versus V plot represents the clearing rate as a function of voltage. The fact that the curve changes slope rapidly above 10 kV is a reflection of chamber size limitations and is explained in Appendix A. The mathematical argument in Appendix A leads to the conclusions that there is increased coalescence in the chamber as a function of increasing voltage, and that pushing becomes more pronounced at high voltages.

B. SLIDES

The slides were separated into three classes: Class I where no voltage was applied to the fog, Class II where measurements were taken after voltage had been applied for 15 seconds and disconnected, and Class III where measurements were taken simultaneously with voltage application. The data taken in all classes were recorded as the number of droplets of a specified size versus time.

The chamber was prefogged for approximately two to four hours. The blotter paper was saturated to ensure the same conditions that were used during the optical measurements.

Voltage (kV)	Reciprocal Time Constant			
	$1/T_{E1}$	$1/T_{E2}$	$1/T_{E3}$	$1/T_{E4}$
0	.011	.011	.010	.010
5	.011	.011	.010	.010
10	.015	.016	.014	.014
15	.026	.022	.023	.023

Table II. Computed reciprocal time constants from optical data for each applied voltage and each section.

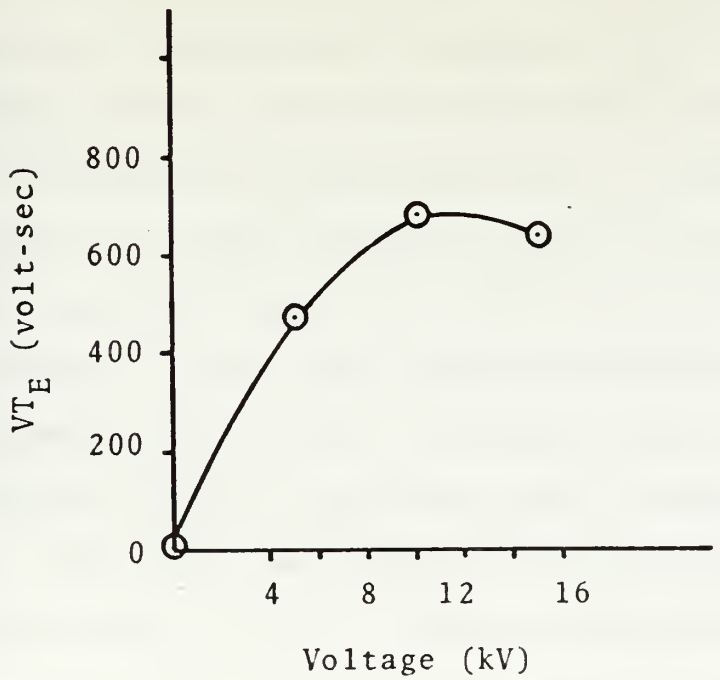

Figure 8. An all-position plot for VT_E versus V. Data for each voltage has been averaged over the four sections.

The blue cloth remained raised and the front glass was not cleared with the blower.

1. Class I

Measurements were taken with the double shutter slide holder (Figure 5). The holder with a freshly prepared slide was placed in the chamber while the spray head was generating fog. The slide holder remained under these conditions for at least five minutes prior to exposure to allow thermal stabilization; then the exposure began. The exposure sequence was as follows: A timer was set for five and a half minutes and the air supply was disconnected at Valve 1 (Figure 1), and the air line from the humidifier to the spray head was also disconnected (Valve 2) to ensure zero flow through the nozzle. Ninety seconds were allowed to elapse prior to exposure of the first section; then the sections of the slide were exposed for 15 seconds with a 30-second interval between exposures. This permitted six exposures per slide. After the first full exposure of a slide, the slide holder was removed and the fog generator reactivated. A new slide and the holder were inserted in the chamber and allowed to stabilize for five minutes; subsequent exposure procedures were the same.

The slides were placed on the microscope and all droplets within a 10 x 10 grid, covering an area on the slide 1.2 mm on a side, were counted using the 10X objective. The droplets were categorized into three sizes: (1) 10μ to 12μ, (2) 25μ and (3) > 25μ. The full slide section was scanned

to ensure no anamolous areas were used; then three 10 x 10 grids were counted per exposed section. The number of droplets counted were averaged and plotted as a histogram of number of similar droplets versus time in seconds. The results are plotted in Figures 9a - o and the data recorded in Table III. Figures 9a - o represent the change in number of droplets counted in each size category at each applied voltage as a function of time.

At the lower (< 10 kV) voltages the only droplets that show a response to the applied voltage are the large (> 25μ) ones. The 10μ and 25μ droplets tend to remain in the fog aggregate in the same numbers for the same length of time. At 10 kV and 15 kV the number of 25μ droplets is reduced and their lifetime decreases as the voltage increases. The 10μ droplets have the same lifetime but their number decreases with increased voltage.

2. Class II

Fog generation was the same as with Class I slides; the fog was allowed to stabilize for 60 seconds, the voltage was turned on for 15 seconds. The voltages used were 2.5 kV, 5 kV, 10 kV, and 15 kV. After 15 seconds the voltage was turned off and 15 seconds elapsed before the first slide exposure was made, corresponding to the 90-second wait for Class I (zero voltage). A measurement taken at zero voltage constituted a standard slide for the measurements taken that day.

10μ Droplets						
Voltage (kV)	time (sec)					
	90	135	180	225	270	315
0	3	23	47	59	66	13
2.5	61	100	105	90	92	63
5.0	45	50	88	46	125	77
10.0	53	79	57	54	57	51
15.0	74	32	35	17	15	24
25μ Droplets						
Voltage (kV)	time (sec)					
	90	135	180	225	270	315
0	128	114	146	48	0	0
2.5	183	140	121	61	0	0
5.0	152	196	144	41	36	0
10.0	81	77	26	15	0	0
15.0	98	22	0	0	0	0
Droplets larger than 25μ						
Voltage (kV)	time (sec)					
	90	135	180	225	270	315
0	94	57	2	0	0	0
2.5	27	16	0	0	0	0
5.0	42	0	0	0	0	0
10.0	55	6	0	0	0	0
15.0	3	0	0	0	0	0

Table III. Average number of droplets recorded on the bottom of the chamber as a function of size and voltage at various times after application of voltage.

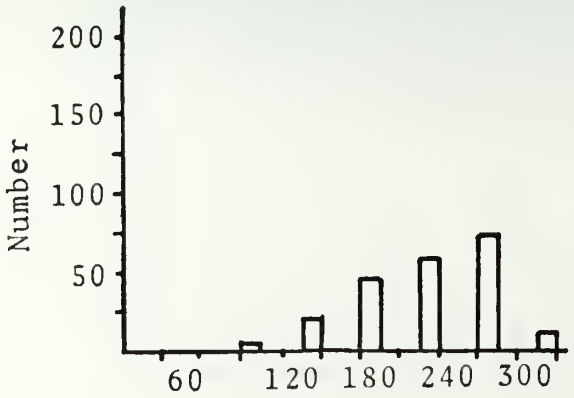

Figure 9a. 10μ droplets at 0 kV.

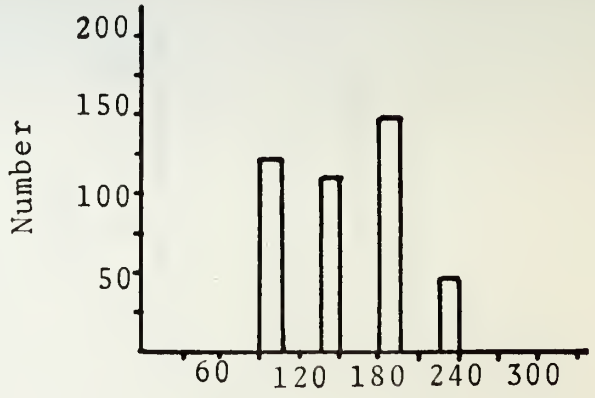

Figure 9b. 25μ droplets at 0 kV.

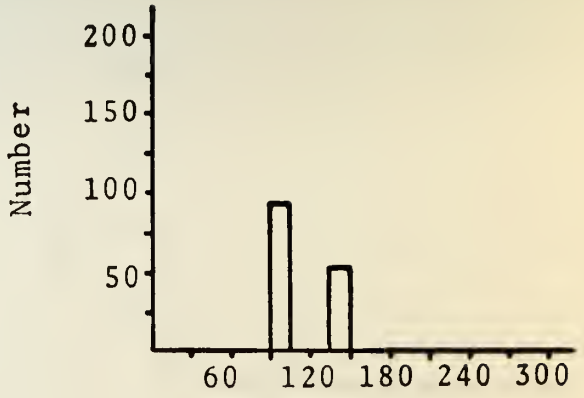

Figure 9c. >25 μdroplets at 0 kV.

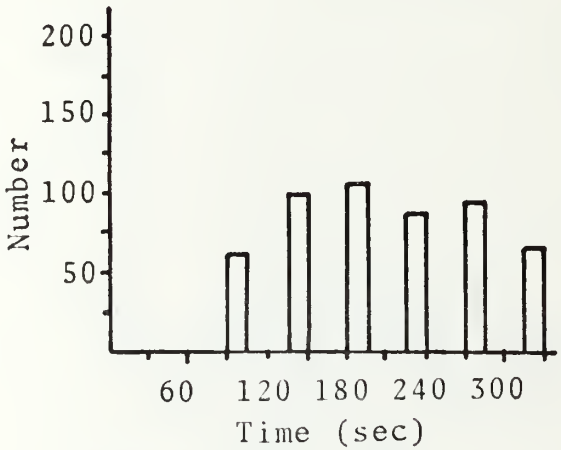

Figure 9d. 10μ droplets at 2.5 kV.

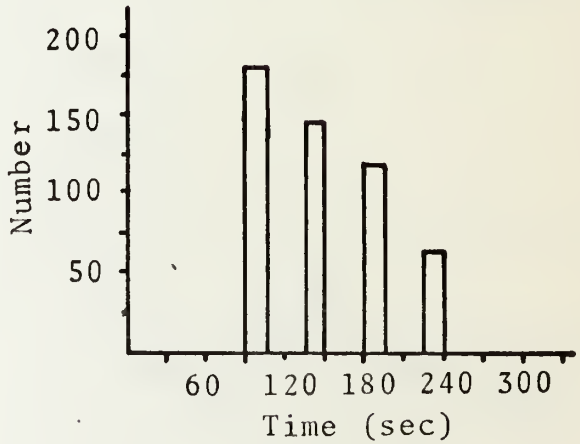

Figure 9e. 25μ droplets at 2.5 kV.

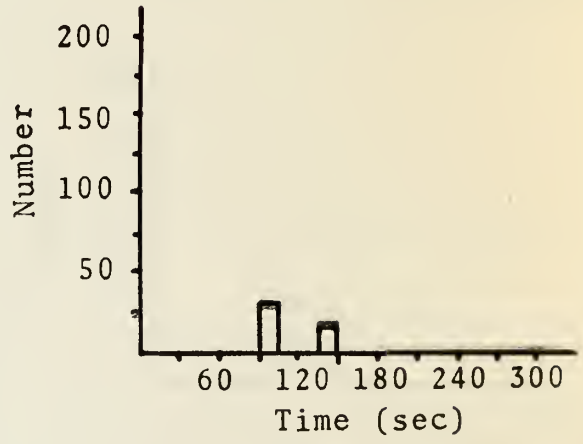

Figure 9f. >25μ droplets at 2.5 kV.

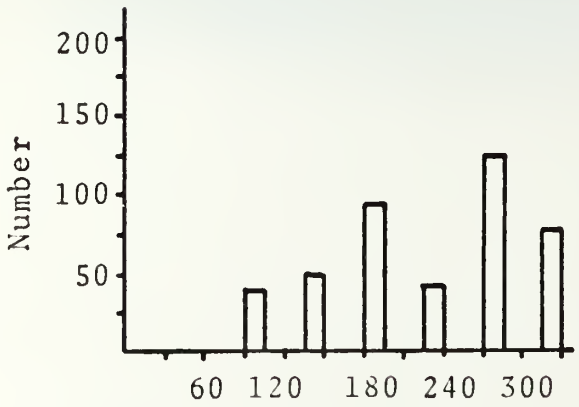

Figure 9g. 10μ droplets at 5.0 kV.

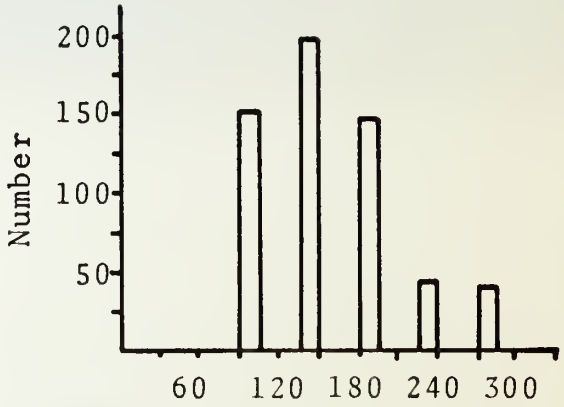

Figure 9h. 25μ droplets at 5.0 kV.

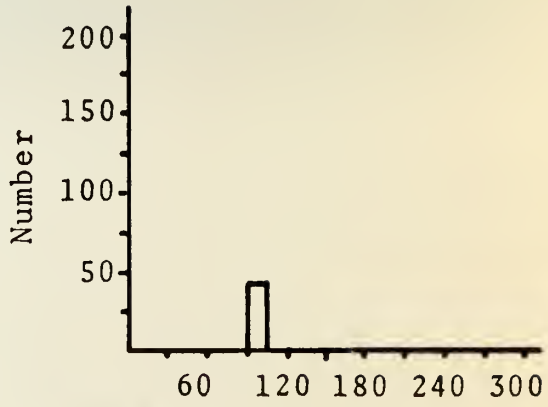

Figure 9i. >25μ droplets at 5.0 kV.

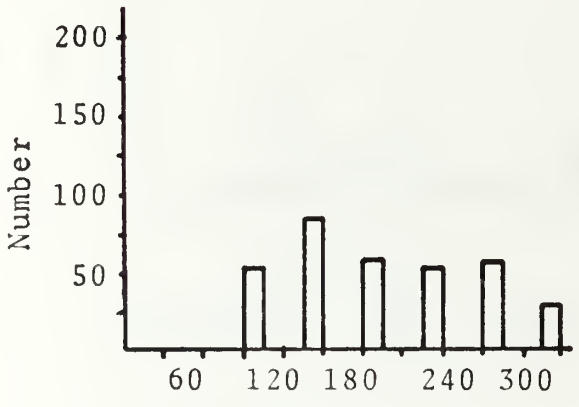

Figure 9j. 10μ droplets at 10.0 kV.

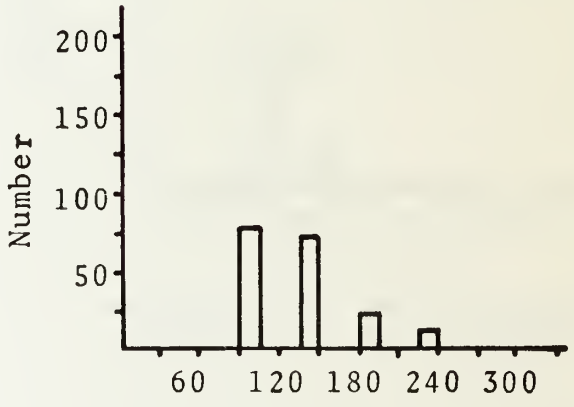

Figure 9k. 25μ droplets at 10.0 kV.

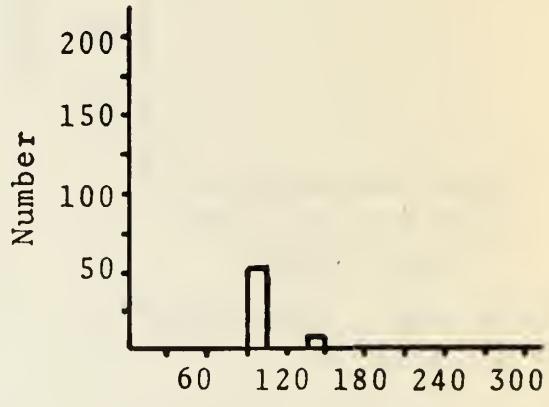

Figure 91. >25μ droplets at 10.0 kV.

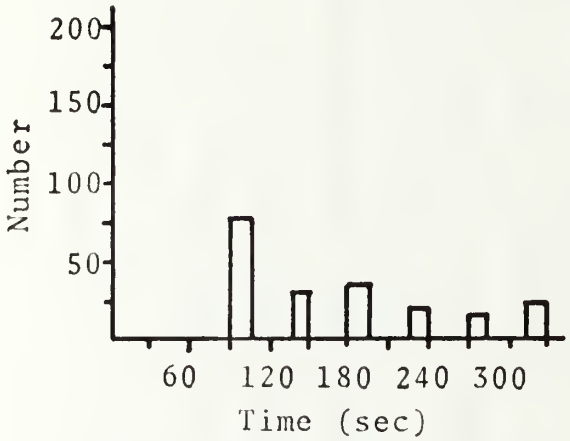

Figure 9m. 10μ droplets at 15.0 kV.

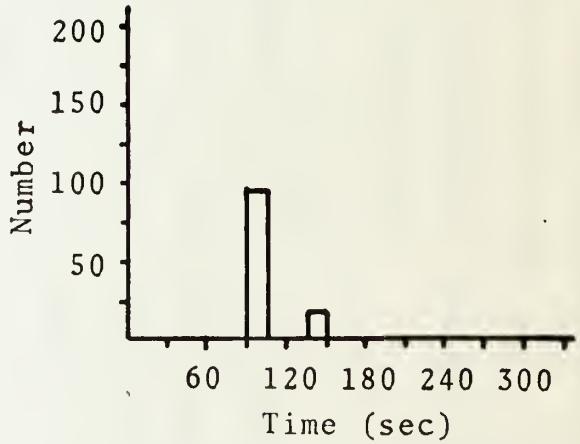

Figure 9n. 25μ droplets at 15.0 kV.

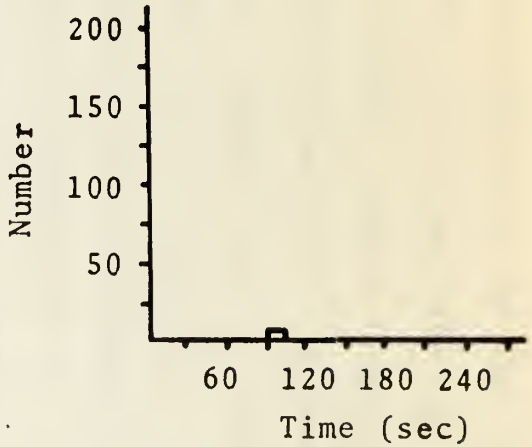

Figure 9o. >25μ droplets at 15.0 kV.

The data were reduced in the same manner as the Class I slides. From the reduced data the droplet size versus time at the specific voltage (Figures 9a - o) and droplet number versus voltage at the various times (Figures 10a - c) was plotted. Figures 10a - c are an illustration of the decrease in the droplet population as a function of voltage and time. These figures represent another view of the data characterized in Figures 9a - o. It shows that the larger droplets are affected the most by voltage with the larger (> 25μ) droplets showing the most response. The average droplet size measurements are tabulated with the Class I measurements (Table III).

3. Class III

The measurements in this class were taken during the application of voltage. Slides were positioned on the bottom of the chamber at points D and F in the plastic holder, and at point G on the side of the chamber in the "coffin." It was necessary to allow the slide holders to come to equilibrium in the fog prior to exposure. The loaded plastic holder was allowed to stabilize in the chamber for at least five minutes with the fog generator on.

Due to the construction of the shutter used on the side of the chamber, the stabilization technique had to be modified. Initially the cardboard holder was placed in the chamber with the fog generating but it was discovered that fog droplets driven by the air would pass through the shutter and impinge upon the slide. This was overcome by allowing

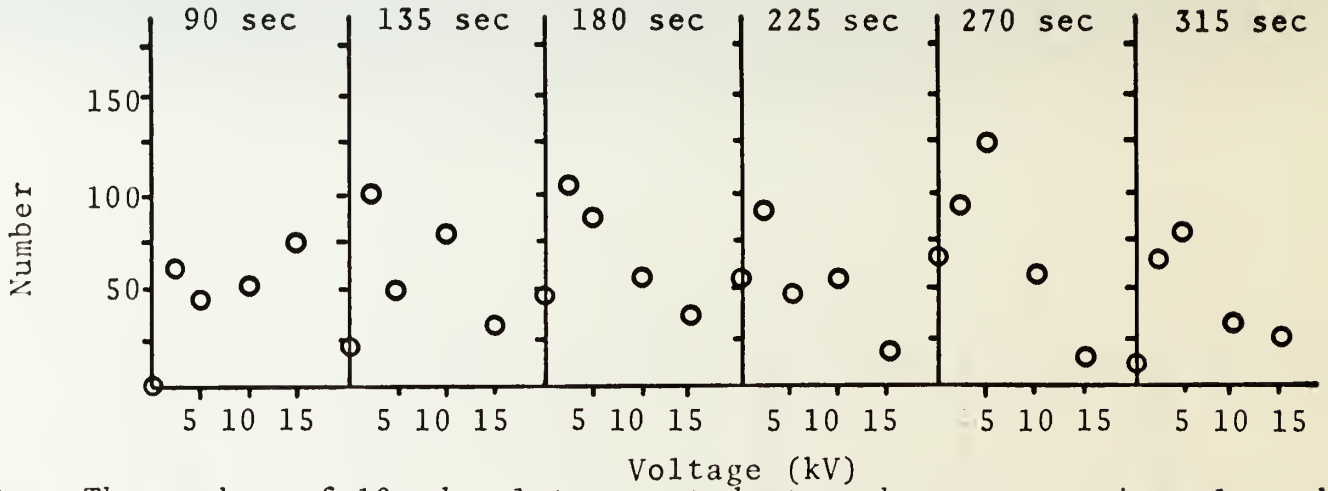

Figure 10a. The number of 10μ droplets counted at each exposure time plotted as a function of applied voltage.

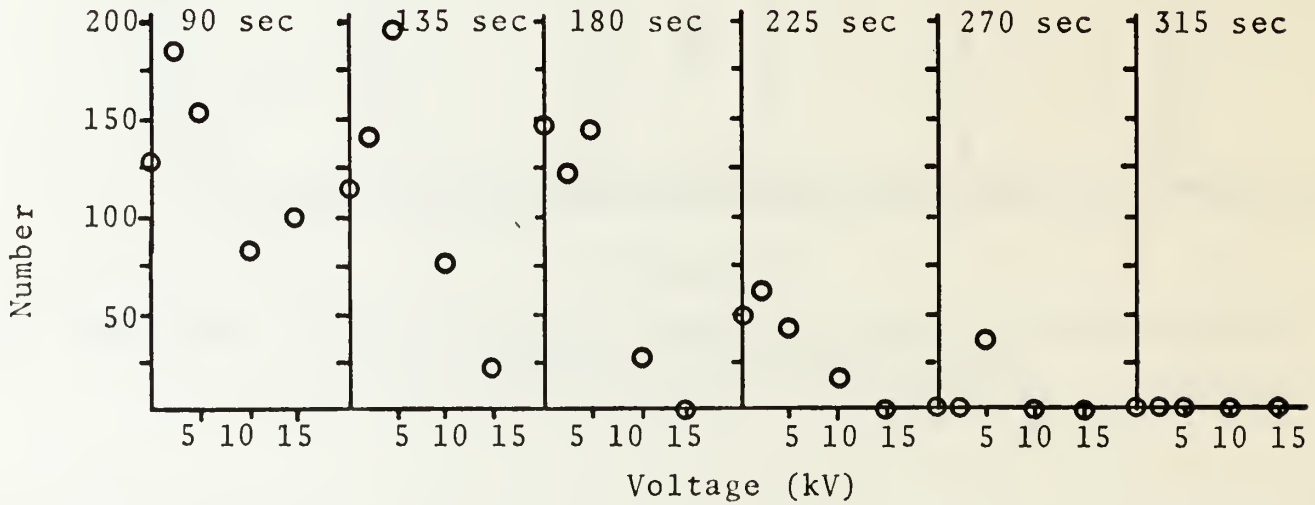

Figure 10b. The number of 25μ droplets counted at each exposure time plotted as a function of applied voltage.

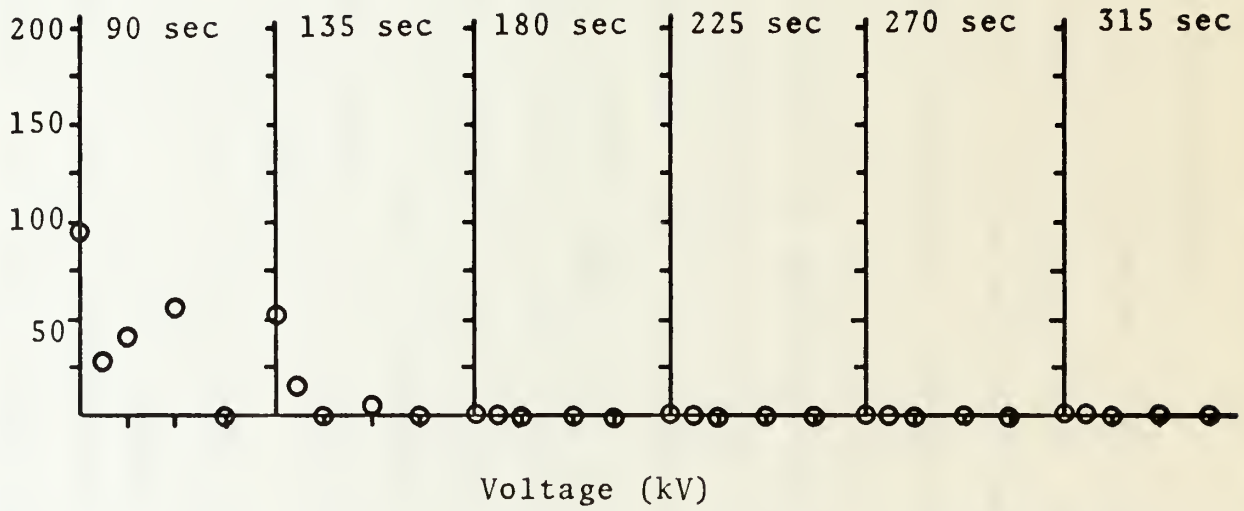

Figure 10c. The number of droplets larger than 25μ counted at each exposure time plotted as a function of applied voltage.

the plastic holder to stabilize normally, shutting the fog off as in Class I, then inserting the coffin holder. This technique allowed a 60-second stabilization time, prior to exposure, for the coffin holder.

A standard set of slides was first exposed for 15 seconds at zero voltage at all locations. After the exposure the chamber was fogged and the holders allowed to stabilize prior to application of voltage. Voltages used were 1.5 kV, 4.9 kV, 9.7 kV and 14.6 kV. The slides were exposed for 15 seconds while the voltage was applied. The slides were scanned over most of their area to ensure that no anomalous conditions were measured. The droplets were divided into six categories: small, droplets 10μ or less which could be the result of a coating that is too thick causing a reduced droplet impression or droplets smaller than 10μ; 25μ; clusters, groups of ten or more 10μ droplets gathered around large droplets (that are not due to random positioning); large, droplets larger than 100μ.

In Table IV data are presented for the total number of droplets at positions, D, F, and G versus applied voltage. The number of droplets recorded at position G was summed regardless of size and the standard, zero-voltage measurement at the same position was subtracted. The resultant data are plotted in Figure 11 and show the increase of droplet number as a function of voltage. Figure 11 represents data recorded at position G and shows that the total number of droplets, regardless of size, increased linearly with

Slide Position	Number of Droplets						Voltage (kV)
	Small	~10μ	~25μ	~50μ	Large	Clusters	
D	21	130	94	7	2	0	1.5
F	22	110	90	14	0	20	
G	8	18	6	20	2	0	
D	26	126	77	2	1	0	4.9
F	10	82	60	35	0	4	
G	15	22	12	5	3	0	
D	25	195	179	6	1	0	9.7
F	23	140	114	11	0	6	
G	--	95	18	4	1	0	
D	26	255	140	0	0	0	14.6
F	24	159	127	17	0	6	
G	--	100	40	4	2	0	

Table IV. Average number of droplets collected at positions D, F, G, during 15-second application of voltage.

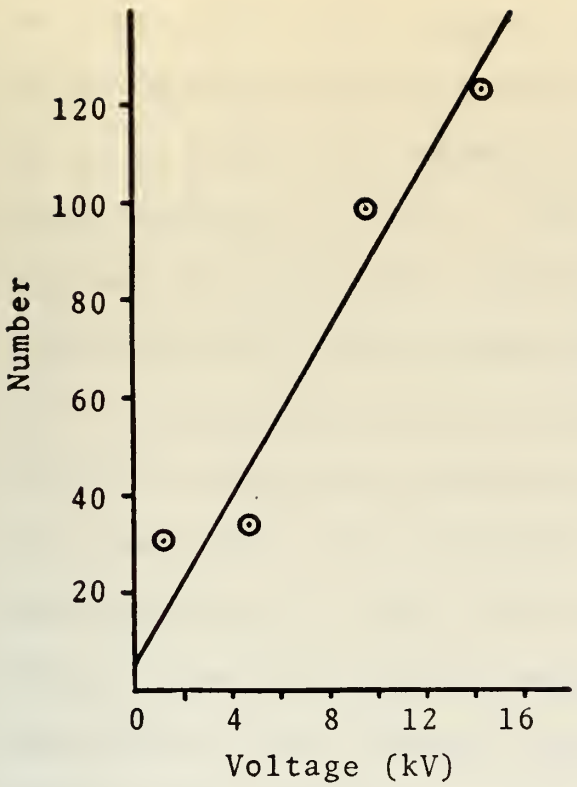

Figure 11. The increase of the total number of droplets at G as a function of applied voltage.

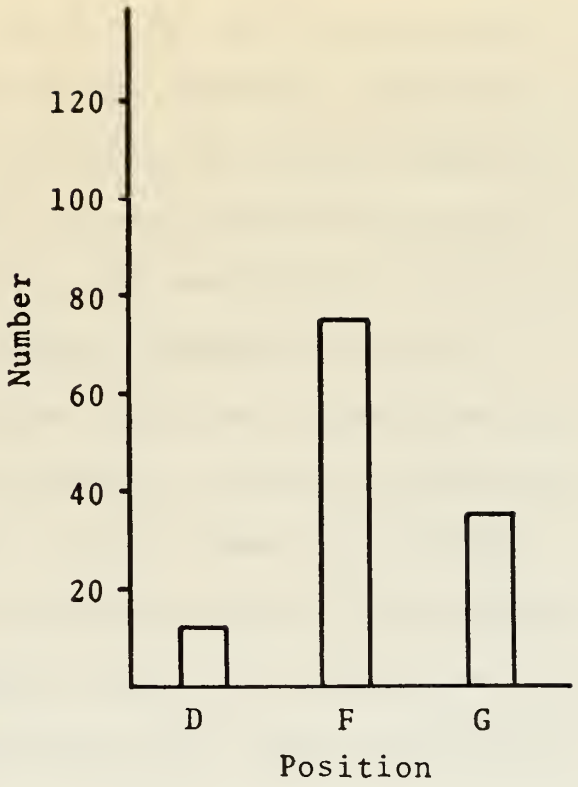

Figure 12a. The total number of 50 droplets as a function of position over all applied voltages.

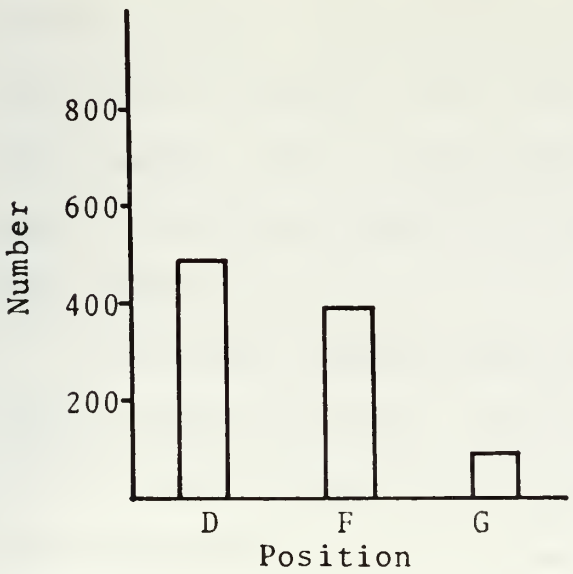

Figure 12b. The total number of 25μ droplets as a function of position over all applied voltages.

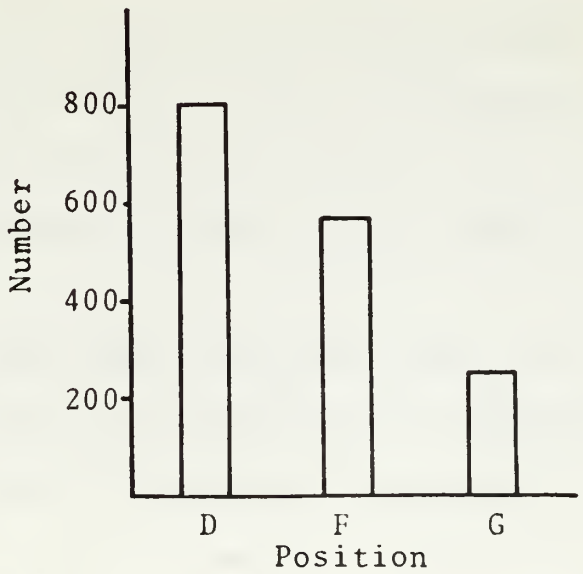

Figure 12c. The total number of 10μ droplets as a function of position over all applied voltages.

voltage. This plot supports the pushing mechanism as one of the dominant forces present in the chamber. Figures 12 a, b, c show the number of droplets of various sizes at three positions, D, F, G. The 10μ and 25μ droplets show a decrease in their total number as the measurement position is moved from the bottom center of the chamber to the side. The 50μ droplets show an increase in number at position F, which is located the furthest distance from the corona head. Position G has also collected a larger number of droplets than position D. These facts indicate that the large (50μ) droplets are experiencing pushing which is driving them from the center of the chamber, indicating that these drops are fairly highly charged.

C. DROPLET CHARGE

Condensation of droplets on the plexiglass window indicated that the droplets entering the chamber were charged by friction in the nozzle. The interaction of droplets so charged with the applied charging field could seriously alter clearing in the chamber. Thus, we measured the charge on droplets as they entered the chamber to determine if this was an important effect.

A one-inch diameter brass electrode was placed about ten inches from the nozzle. The rate at which water was collected on the electrode and the electrical current were measured simultaneously. It was assumed that the water arrived at the electrode as 20μ droplets. The number of droplets per

unit time arriving at the electrode was thus determined and, from this value and the current, the charge per droplet was found. The results for the metal and the plastic nozzle are as follows:

1. Metal Nozzle

Water collection rate at electrode:	4.3 g/min
Current measured:	$+2.8 \times 10^{-9}$ amp
Water flow rate through nozzle:	31.3 g/min
Charge on 20μ droplet:	4×10^{-16} Coul/drop

2. Plastic Nozzle

Water collection rate at electrode:	4.9 g/min
Current measured:	$+4 \times 10^{-10}$ amp
Water flow rate through nozzle:	9.6 g/min
Charge on 20μ droplet:	2×10^{-17} Coul/drop

If we assume a 10 kV potential difference between flat plates separated electrically by 0.5 meter, we grossly approximate the field conditions of the fog chamber. Using the assumption of a 20μ droplet size we find, through a simple computation, that this electric field gives an acceleration of 10^{-3} m/sec to the droplets, which is much less than that due to gravity. To obtain the clearing effect we observe with the application of high voltage, the droplets must be much more highly charged, presumably collecting charge from the corona discharge.

D. TEMPERATURE

Measurements were taken in two different manners: (1) glass centigrade thermometers and (2) thermocouples.

The measurements recorded with the glass thermometers were taken inside and outside the chamber simultaneously. The temperature inside the chamber was usually 2° cooler than the temperature outside.

The thermocouple measurements were taken at three points inside the chamber (Figure 2). A series of measurements with no fog in the chamber, during fog production, and during dissipation showed no appreciable difference (less than .2° C) in temperature at the three points. It was concluded that a significant temperature gradient did not occur in the chamber.

The electrostatic repulsion of the water droplets charged by the corona discharge rapidly decreased the density of the fog in the center of the chamber. This density reduction occurs radially outward until confined by the chamber walls. The optical measurements were recorded at positions well away (at least six inches) from the walls so the only phenomenon recorded was the change of the time constant, Table II.

The dipolar attraction of the water droplets is also present during voltage application. This phenomenon occurs around the lead wire and serves to increase the density of the fog in that area. Some of the slide measurements, Figures 9a - o, were taken at the base of the lead-in wire and would reflect this increased density with a higher number of droplets appearing in the initial exposures after the application of voltage.

More supportive evidence for the model is illustrated in Figure 11 which shows the ratio of the number of 10μ droplets at 2.5 kV to the number at 0 kV, as a function of time. The figure shows the ratio starting high and dropping off as a function of time, the last measurement in the series showing a rise. This behavior would correspond to the initial highly dense layer of droplets near the electrode at the bottom of the chamber falling on the slide, followed by the lesser density of droplets from the center of the chamber. The sudden rise is an indication of the larger density of droplets at the top of the chamber.

V. CONCLUSIONS

A. GENERAL

The most readily observed indication of the dispersal of fog is increased visibility. Thus, the first experiments performed were optical. Direct visual observation and quantitative optical measurements showed that the fog in the chamber dissipated much more rapidly under the application of high voltage. The optical measurements were consistent with both clearing by coalescence, evaporation, or by pushing the fog to the walls of the chamber. It was not possible to determine which, if any, of the mechanisms is dominant.

Slides are a more useful measurement tool for this type of experiment since they provide a determination of the number of droplets and of the droplet size distribution. The slides allowed us to reject enhanced evaporation as a clearing mechanism since the number of small droplets observed was not increased under the application of voltage. In fact, the results tended to show that the larger droplets are those that are charged, which indicated coalescence. Also, measurements made with slides placed at various positions in the chamber showed definite evidence of pushing of the fog droplets to the walls.

At the present state of this work we have definite evidence that the following mechanisms are occurring in the chamber:

1. Changing of droplets by corona - leading to coalescence.

2. Changing of droplets by corona - the charged droplets then being pushed to the walls.
3. Clustering of droplets about larger charged droplets.
4. Attraction of droplets to the charging electrode structure through an induced dipole moment.

There is no experimental evidence that allows identification of a dominant clearing mechanism, which is undoubtedly due to the small size of the fog chamber. A larger chamber would allow much better separation and observation of the various mechanisms. The various mechanisms and the experimental evidence for them will be discussed in detail below.

B. DISCUSSION OF EXPERIMENTAL RESULTS

Since the experiments dealt with the time decay of a natural phenomenon, it was felt that the effects should occur exponentially with time, the time constant changing with voltage application. The optical measurements, Figure 7, followed this expectation but the slides did not seem to. Figures 9a - o, the histograms of droplet number versus time as a function of voltage, showed some decay but not exponential. This unexpected behavior cannot be resolved through experimental error. It is apparent that application of high voltage is causing a non-uniform fog distribution in the chamber. This model is described below.

1. Fog Chamber Behavior Model

The application of voltage causes an anomalous fog distribution within the chamber through two mechanisms:

(1) electrostatic repulsion and (2) dipolar attraction. Figure 13 is a pictoral representation of the physical forces that seem to be operating.

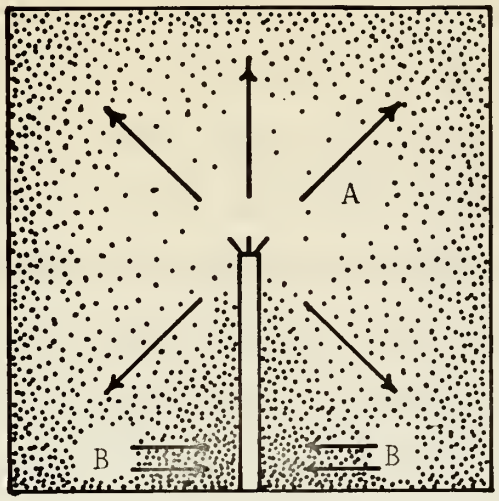

Figure 13. Fog chamber model illustrating
A. corona charging and pushing and
B. dipolar attraction.

The electrostatic repulsion of the water droplets by the conora discharge rapidly decreased the density of the fog in the center of the chamber. This density reduction reacted radially outward until confined by the chamber walls. The optical measurements were recorded at positions well away (at least six inches) from the walls so the only phenomenon recorded was the change of the time constant, Table II.

The dipolar attraction of the water droplets is also present during voltage application. This phenomenon occurs around the lead wire and serves to increase the density of the fog in that area. Some of the slide measurements,

Figures 9a - o, were taken at the base of the lead wire and would reflect this increased density with a higher number of droplets appearing in the initial exposures after the application of voltage.

More supportive evidence for the model is illustrated in Figure 14 which shows the ratio of the number of 10μ droplets at 2.5 kV to the number at 0 kV. The figure shows that the ratio starts high and decreases as a function of time. The last measurement in the series shows a slight rise. This behavior would correspond to the initial dense layer of droplets that fall on the slide, followed by the decreasing density of droplets from the center of the chamber. The sudden rise is an indication of the dense droplets that were forced radially outward to the top of the chamber.

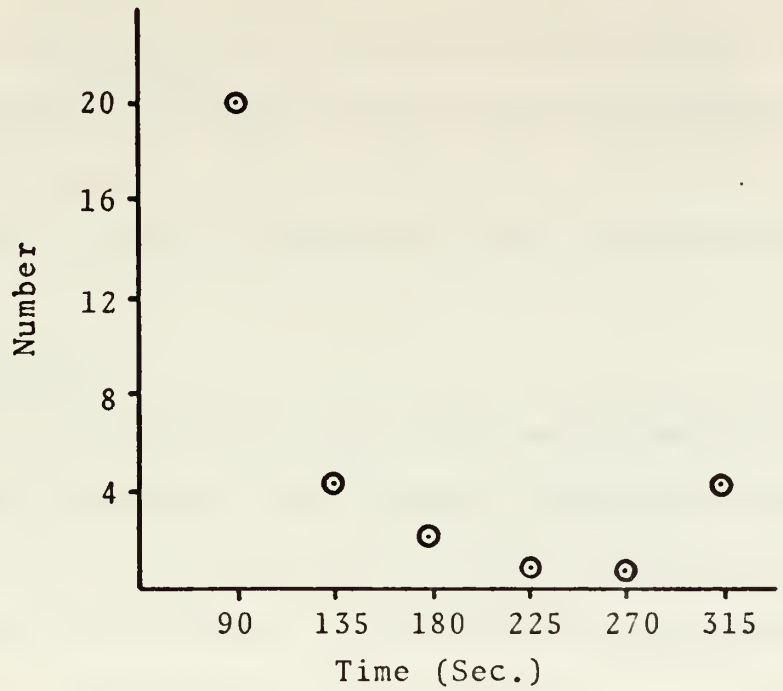

Figure 14. The ratio of the number of 10μ droplets at 2.5 kV to the number of 10μ droplets at 0 kV at each exposure time at position (D).

2. Optical

Figure 7 illustrates the fact that as the voltage is increased, the rate of fog dispersal increases. The basic data does not support ideas concerning the exact mechanism for clearing but a VT_E versus V plot (Figure 8) does lead to some interesting conclusions. The mathematical argument is presented in Appendix A. The mathematical argument leads to the result that $VT_E = \frac{K}{\mu}$, where K is a constant, and μ is the mobility. Figure 7 shows an increase in VT_E as the voltage is increased indicating a decrease in μ.

As the voltage is increased, the mobility decreases which is a fairly clear indication that the droplet mass increases by coalescence. From Figure 8, we see that the curve does drop (within experimental error) at high voltage which is consistent with the pushing phenomenon. Once the electrostatic repulsion from the corona head becomes too large, the droplets move so fast that, within the confines of the small chamber, coalescence does not have time to occur.

3. Slides

It was hoped that the slide measurements would lead to an identification of the dominant clearing phenomena. This was not the case and the measurements only supplied more supportive evidence of pushing and coalescence.

a. Coalescence and Clustering

Figure 15a is a photograph of a slide section exposed during a 2.5 kV application. A preponderance of

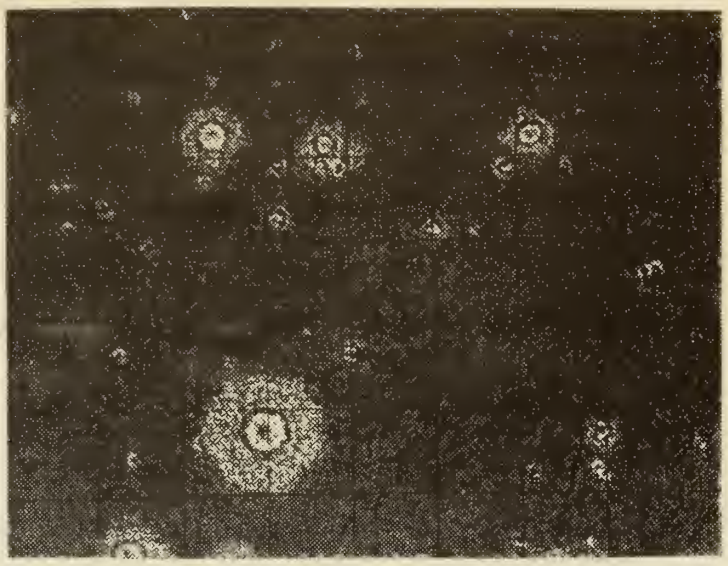

Figure 15a. Photograph of the slide at position G exposed during a 15-second application of 1.7 kV showing large droplets.

the number of droplets that appeared on the low voltage slides was larger than the droplets that appeared on the zero voltage or the higher (5 kV - 15 kV) voltage slides (Figure 15b). These large (> 100μ) droplets seemed to be a function of position in the chamber and the greatest number collected was at position G, on the side of the chamber. These droplets apparently had undergone collision and coalescence prior to their arrival at the slide.

It was also noted that position F, the slide furthest from the corona head, collected most of the clusters (Figure 15c). The clusters could be droplets that have collected but not coalesced or multiple overlapping impacts on the slide. The clusters appear around the large (> 100μ) droplets and would tend to suggest that the larger droplets were charged. This charge would increase the collection efficiency and the small size of the chamber could be a reason for the lack of coalescence. Also, if a larger droplet on a slide were charged, it would tend to increase the number of smaller droplets that would impact in the same area of a slide because of dipolar attraction.

b. Pushing

Measurements recorded on the side of the chamber (position G) during voltage application (Class III) are illustrated in Figure 11 and illustrate the pushing of charged droplets. The total number of droplets collected increases directly with high voltage application. It was also noted that slides exposed after voltage application

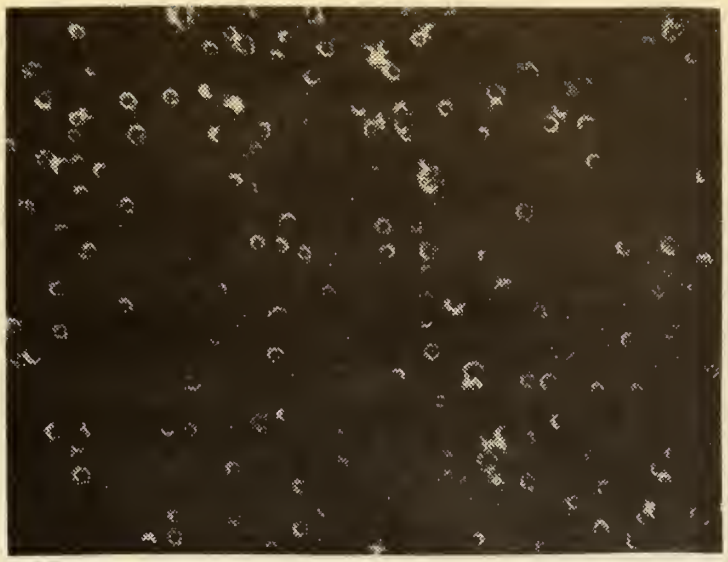

Figure 15b. Droplets collected at 14.7 kV at position G. Note the absence of large droplets.

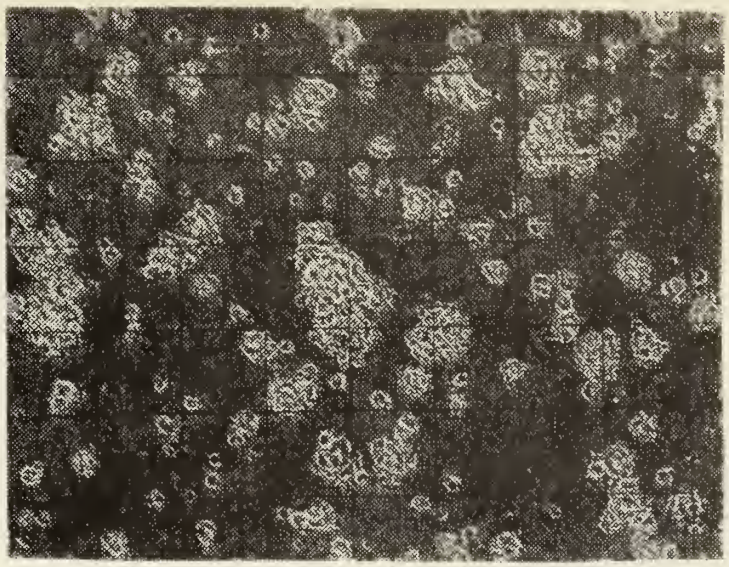

Figure 15c. The clustering phenomenon that occurred at position F regardless of applied voltage.

(Class II) showed a reduced number of larger (> 25μ) droplets than zero voltage slides under the same conditions (Figures 9a - o). Evidently large, 25μ, droplets can become more highly charged than the smaller droplets and are preferentially swept to the walls by pushing. This preferential sweeping would reduce the number of large droplets suspended in the fog.

The movie taken of the fog chamber in operation under voltage application shows a dramatic illustration of pushing. When the voltage was applied, turbulence could be seen around the corona head and the fog cleared from the head radially outward. Pushing is definitely present in the chamber, but its relative importance in relation to coalescence is unknown.

VI. RECOMMENDATIONS

To date the laboratory experiments have not been completely adequate in studying the physical effects of inserting charge into fog as a clearing mechanism. It is felt that further investigation into this area should proceed with the following suggestions in mind. The recommendations should enable clarification of the physical phenomenon occurring during application of high voltage.

1. The major limitation in the experiment was the small size of the chamber; a larger (room sized) chamber would enable more definitive measurements. A larger chamber would help clarify the distance dependence of the phenomenon and allow more conclusive tests concerning the relative importance of pushing and coalescence.

2. The slide measurements of the fog droplets produced by the spray nozzle showed a size distribution between 10μ and 50μ. It is felt that more control over the size distribution of the droplets produced would afford more definitive measurements to be made. A further literature search gave information on a spinning disk atomizer (Ametin, 1967; May, 1950) which produced droplets that are within 5% of the mean size. The mean size of the droplets is controlled by the rotational speed of the disk. This atomizer would have to be investigated to find if the quantity of droplets produced would be adequate for chamber use.

3. Evidence taken with slides seems to allude to the idea that the larger droplets were preferentially gaining charge during voltage application. The charge measurements performed in this research were on the fog from the nozzle without any applied voltage. It is felt that the droplet charge needs to be measured at all phases of the dissipation process: (1) no voltage, (2) after voltage application, and (3) during voltage application. These measurements would determine the magnitude of charging of various sized droplets which could be critical information as far as warm fog dissipation is concerned.

4. The coated slide technique seems to be the most conclusive method for droplet size and distribution sampling. Good results were obtainable with the MgO coating but its thickness was critical. May (1945) stated that the MgO thickness should be the same as the diameter of the droplets being measured. It was also pointed out by May (1950) that due to the particle size of the MgO, droplets smaller than 10μ would be lost. More information would be obtained if a slide coating that would resolve droplets from 1μ to 200μ were used. Ease of application and simplicity of droplet measurement would be the main criteria considered in the use of a new coating.

5. A more efficient method for gathering the smaller (1 - 10μ) droplets is through the use of a cascade impactor (May, 1945, 1961). This equipment should be investigated for possible adaption to the fog chamber experiments.

6. The slide measurements in the chamber were limited to two positions: bottom and side. A better technique would be the measurement of the droplets at a variety of positions around the interior of the chamber, not limited to points adjacent to the walls.

APPENDIX A

MOBILITY

The fog droplets in the chamber are in a state of random thermal motion and drift to the bottom of the chamber due to the gravitational force. As they drift, the visibility in the chamber clears exponentially with time. We will call the time constant associated with clearing for this case T_o. When the voltage is applied the chamber clears much more rapidly, the clearing again being exponential with time. The time constant for this case will be identified as T_E.

For random droplet motion with diffusion the mean free path is given by:

$$\ell_o = (D\tau)^{1/2} , \qquad (1)$$

where D is the diffusion constant and τ the mean free time. The diffusion constant can be related to the mobility μ and the temperature T using the Einstein relation:

$$D = \kappa T\mu . \qquad (2)$$

κ is the Boltzman constant.

If an electric field is applied, the force on a droplet with charge q will be qE. In this case, the mean free time and mean free path are related by:

$$\ell = \mu q E \tau \ , \qquad (3)$$

where we have assumed the electric field produces the dominant effect.

The mean free time will not be changed by the application of the electric field. We now relate these parameters to the observed optical decay times. The optical decay times can be related to the mean free time through an unknown characteristic length, ℓ_c, as

$$\frac{T_o}{\tau} = \frac{\ell_c}{\ell_o} \ ,$$

$$\frac{T_E}{\tau} = \frac{\ell_c}{\ell} \ .$$

Thus,

$$\frac{T_E}{T_o} = \frac{\ell_o}{\ell} = \frac{\sqrt{\mu \kappa T \tau}}{\mu q E \tau} \ . \qquad (4)$$

We assume the elctric field can be calculated from the applied potential V and a length L, characteristic of the geometry of the chamber: E = V/L. Making this substitution and solving for VT_E we find:

$$VT_E = \frac{L \ T_o}{q} \left(\frac{\kappa T}{\mu \tau}\right)^{1/2} \ . \qquad (5)$$

All quantities on the right-hand side are constant with the exception of μ, and possibly q. If the droplets obtain their

charge from the corona discharge it is reasonable to assume that some maximum charge will be quickly reached while the droplets are in the discharge, because of electrostatic repulsion. Thus, assuming constant charge, we have

$$VT_E = (\text{constant})\ (\mu)^{-1/2} \ . \qquad (6)$$

T_E is determined directly from optical measurements and the product VT_E gives a measure of droplet mobility as a function of voltage. A decrease of mobility with applied voltage is a good indication of charge-induced coalescence.

APPENDIX B

FOG CHAMBER CONSTRUCTION

Since a great deal of time and effort were expended on the construction of the fog chamber, it was felt that information concerning its development is beneficial for future undertakings. A stable, easily cycled chamber is essential in any laboratory fog study. It is felt that the following construction parameters must be met to produce a workable laboratory fog chamber:

1. A moisture-retaining material must be present in the interior of the chamber to maintain the high degree of saturation necessary for fog.

2. Even though steam produces a fog that closely resembles natural fog in size of droplets and density, the condensation problem precludes its use during optical measurements. (The use of an atomizer eliminates the condensation problem.)

3. The use of humidified air when using a nozzle precludes the introduction of a large volume of "dry air" into the chamber, thus reducing the evaporation rate of the smaller droplets.

4. If the atomizer is air-driven, its design should be such that the largest number of droplets per volume is produced; a spray nozzle achieves this effect.

LIST OF REFERENCES

Aberth, W., C. A. Spindt, and K. T. Rogers, 1971: Multipoint field ionization beam source. Paper presented at 11th symposium on Electron Ion and Laser Beam Technology, Boulder, Colorado.

Amerlin, A. G., 1967: Theory of Fog Condensation, 2 ed., Israel Program for Scientific Translation, Jerusalem, 43-58.

Arthur D. Little, Inc., 1956: Warm fog and stratus cloud dissipation. Final report to Signal Corps, Contract DA-36-039 SC-64569, ASTIA AD-204 315, Cambridge, Massachusetts.

Cadle, R. D., 1955: Particle Size Determination. Interscience Publishers, Inc., New York, 1-147.

Cochet, R., 1951: Meteorology - formation of charged water droplets in clouds and fog at positive temperature. Translated by Emmanual College Research Language Center, Contract AF 19(628) - 3869, Air Force Cambridge Research Laboratories, Bedford, Massachusetts.

Cong, J. Luan Phan and Phuoc Dinh-Van, 1972: Direct measurement of coalescence efficiency and frequency of small water droplets in an electric field. Tellus, 25, 63-68.

Cong, J. Luan Phan and Jan B. Jordan, 1969: Fog droplets in electrostatic field. IEEE Trans. on Geoscience Electronics, GE-7, 250-252.

Cong, J. Luan Phan and J. B. Jordan, 1970: The influence of electric charge and field upon fog modification. Paper presented at the Second National Conference on Weather Modification, Santa Barbara, California, 6-9 April.

Department of the Navy, 1973: OPNAV Instruction 3710.7G. Office of the Chief of Naval Operations, Washington, D.C.

Dolezalek, H., 1962: Atmospheric electric parameter study - Survey on an effect relating atmospheric electric variation with formation and dissipation of fog. Final Rept., RAD-TR-62-32 by Avco Corp., Contract None 3388(00), Office of Naval Research, Washington, D.C.

Golikov, V. I., 1961: Device for measuring the size spectrum of spherical particles and fog droplets. Transl. Rept. 422, Contract AF 19(628)-3880, ASTIA AD-602 187, Amer. Meteor. Soc., Boston, Massachusetts.

Gourdine, M. C., 1971: Preliminary design of an airport fog dispersal system, TM-1206-MCG, Gourdine Systems, Inc.

Gourdine Systems, Inc., 1972: Proposal for an electrogas-dynamic fog dispersal system for airports. P1128.

Green, H. L., and W. R. Lane, 1964: Particulate clouds: Dusts, Smokes, and Mists, 2 ed. D. Van Nostrand Company, Inc., Princeton, 410-437.

Hamilton, G. D., 1963: Atmospheric electricity measurements as a possible aid in fog forecasting. NWRF 29-1263-086, DDC AD-431 763, U. S. Navy Weather Research Facility, Norfolk, Virginia.

Hagen, G. E., 1961: Study, development and testing of a fog clearing device. Rept. No. 3 (Final), Contract DA-36-039 SC-84962, ASTIA AD-270 850, Island Research, Inc.

Herdan, G., 1953: Small Particle Statistics. Elsevier Publishing Company, New York, 434-444.

Houghton, H. G., and W. H. Radford, 1938A: On the local dissipation of natural fog. Papers in Physical Oceanography and Meteorology, Vol. 6, No. 3.

Houghton, H. G., and W. H. Radford, 1938B: Microscopic measurement of the size of natural fog particles. Papers in Physical Oceanography and Meteorology, Vol. 6, No. 3, 5-18.

Huschke, R. E. (ed.), 1959: Glossary of Meteorology. Amer. Meteor. Soc., Boston, Massachusetts, 227.

Irani, R. R. and Clayton F. Callis, 1963: Particle Size: Measurement, Interpretation, and Application. John Wiley and Sons, Inc., New York, 93-106.

Juisto, J. E., 1972: Laboratory evaluation of an electro-gasdynamic fog dispersal concept. (Final Report), Atmospheric Sciences Research Center, Contract WI-73-0077-1, FAA-RD-72-99. Federal Aviation Administration, Washington, D. C.

Jiusto, J. E., 1964: Project fog drops - investigation of warm fog properties and fog modification concepts. (First Annual Summary Report), Cornell Aeronautical Laboratory, Inc., Contract NASR-156 MASA CR-72, National Aeronautics and Space Administration, Washington, D. C.

Junge, C. E., 1958: Methods of artificial fog dispersal and their evaluation. AFCRC-TN-58-476, ASTIA AD-160 751, AF Surveys in Geophysics No. 105, Air Force Cambridge Research Center, Bedford, Massachusetts.

Kottler, F., 1952: The logarithmico - normal distribution of particle sizes, homogeneity and heterogeneity. J. of Phys. Chem., 56, 442.

Latham, J., and I. W. Roxburgh, 1966: Disintegration of pairs of water drops in an electric field, R. Soc. London Proc. A, 295, 84-97.

Lieberman, A., 1960: Warm fog and cloud dissipation. Final Rept. ARF 3153-6, Armour Research Foundation, Contract AF 19 (604)-5910, ASTIA AD-254 489, AFCRL 260, Air Force Cambridge Research Lab., Bedford, Massachusetts.

Loveland, R. B., et al., 1972: Project foggy cloud IV - Phase II warm fog modification by electrostatically charged particles. NWC TP 5338, Ecom 5426, Naval Weapons Center, China Lake, California.

MacCready, P. B., Jr., and T. R. Mee, 1965: Weather modification for Naval applications. Rept. MRI 65-FR-266, Contract N 189 (188) - 58768A, ASTIA AD-478 176, for U. S. Navy Weather Research Facility, Norfolk, Virginia.

Marchetti, M. J., 1972: Laboratory experiments on warm fog dissipation. Master's Thesis, U. S. Naval Postgraduate School, Monterey, California.

Mason, B. J., 1971: The Physics of Clouds, 2 ed., Clarendon Press, Oxford, 382.

May, K. R., 1961: Fog-droplet sampling using a modified impactor technique. Quart. J. R. Meteor. Soc., 87, 535-548.

May, K. R., 1945: The cascade impactor - an instrument for sampling coarse aerosols. J. Sci. Instr. 22, 187-195.

May, K. R., 1950: The measurement of airborne droplets by the magnesium oxide method. J. Sci. Instr., 27, 128-130.

Owens, T., 1961: Warm fog dispersal methods and fog characteristics at Monterey, California. Master's Thesis, U. S. Naval Postgraduate School, Monterey, California.

Pauthenier, M., 1950: Electrical coalescence of fog and clouds. Cent. Proc. R. Meteor. Soc., 60-61.

Pilié, R. J., 1966: Project fog drops - investigation of warm fog properties and fog modification concepts. (Second annual summary report), Cornell Aeronautical Laboratory, Inc., Contract NASR-156, NASA CR-368, National Aeronautics and Space Administration, Washington, D. C., 50-54.

Pilié, R. J., and W. C. Kochmond, 1967: Project fog drops - investigation of warm fog properties and fog modification concepts, Vol. III (third annual summary report), Cornell Aeronautical Laboratory, Inc., Contract NASR-156, MASA CR675, National Aeronautics and Space Administration, Washington, D. C., 36-46.

Plumlee, H. R., 1964: Effects of electrostatic forces on drop collision and coalescence in air. rept. CPRL-8-64, Grants AMC-63-G2 and NSF GP-2528, Charged Particle Research Lab., Univ. of Illinois, Urbana, Illinois.

Radford, W. H., 1938: An instrument for sampling and measuring liquid fog water, Pap. Phys. Ocean. Meteor., 6, 19-31.

Sartor, J. D., 1960: The role of the electrostatic field in the coagulation of fog and cloud droplets. Report P-2134, The Rand Corp., Santa Monica, California.

Sartor, J. D., 1972: Clouds and precipitation, Physics Today, 25, 32-38.

Schulepov, Yu. V., and S. S. Sukhin, 1963: In reference to the theory of electrical coagulation of spherical aerosol particles. Kolloidnzy Zhirual, 24, 749 (translation A. F. Foreign Technology Division Report M. T. - 63-70).

Vonnegut, B., and C. B. Moore, 1958: Preliminary attempts to influence convective electrification in cumulus clouds by the introduction of space charge into the lower atmosphere. Conf. on Atmos. Elect., Wentworth-by-the-Sea, N. H., A. D. Little, Inc., Cambridge, Massachusetts.

Voniegut, B., Duncan C. Blanchard, and Robert A. Cudney, 1969: Structure and modification of clouds and fogs. Annual summary report No. 2. Research Foundation of State University of New York, Contract F 19628-68-c-0057, AFCRL-69-0513, Air Force Cambridge Research Lab., Bedford, Massachusetts.

Vonnegut, B., et al., 1967: Technique for the introduction into the atmosphere of high concentrations of electrically charged aerosol particles. J. Atmos. Terrestrial Physics, 29, 781-792.

INITIAL DISTRIBUTION LIST

		No. Copies
1.	Defense Documentation Center Cameron Station Alexandria, Virginia 22314	2
2.	Library, Code 0212 Naval Postgraduate School Monterey, California 93940	2
3.	Department Chairman, Code 61 Department of Physics and Chemistry Naval Postgraduate School Monterey, California 93940	2
4.	Assoc Professor G. E. Schacher, Code 61 Sq Department of Physics and Chemistry Naval Postgraduate School Monterey, California 93940	10
5.	Assoc Professor W. Reese, Code 61 Rc Department of Physics and Chemistry Naval Postgraduate School Monterey, California 93940	2
6.	Professor Dale Leipper, Code 58 Lr Department of Oceanography Naval Postgraduate School Monterey, California 93940	1
7.	Assoc Professor Charles Taylor, Code 51 Ta Department of Meteorology Naval Postgraduate School Monterey, California 93940	1
8.	Dr. Pierre St. Amand Earth and Planetary Sciences Naval Weapons Center China Lake, California 93527	2
9.	Dr. Paul Tag Environmental Prediction Research Facility Naval Postgraduate School Monterey, California 93940	1

10. Dr. Richard Clark — 1
Earth and Planetary Sciences
Naval Weapons Center
China Lake, California 93527

11. Capt L. B. Herman, USMC — 2
4625 68th Street
San Diego, California 92115

UNCLASSIFIED

SECURITY CLASSIFICATION OF THIS PAGE *(When Data Entered)*

REPORT DOCUMENTATION PAGE		READ INSTRUCTIONS BEFORE COMPLETING FORM
1. REPORT NUMBER	2. GOVT ACCESSION NO.	3. RECIPIENT'S CATALOG NUMBER
4. TITLE *(and Subtitle)* Laboratory Investigation of Electrical Dissipation of Warm Fog		5. TYPE OF REPORT & PERIOD COVERED Master's Thesis; December 1973 6. PERFORMING ORG. REPORT NUMBER
7. AUTHOR(s) Leslie Bruce Herman		8. CONTRACT OR GRANT NUMBER(s)
9. PERFORMING ORGANIZATION NAME AND ADDRESS Naval Postgraduate School Monterey, California 93940		10. PROGRAM ELEMENT, PROJECT, TASK AREA & WORK UNIT NUMBERS
11. CONTROLLING OFFICE NAME AND ADDRESS Naval Postgraduate School Monterey, California 93940		12. REPORT DATE December 1973 13. NUMBER OF PAGES 94
14. MONITORING AGENCY NAME & ADDRESS*(if different from Controlling Office)* Naval Postgraduate School Monterey, California 93940		15. SECURITY CLASS. *(of this report)* Unclassified 15a. DECLASSIFICATION/DOWNGRADING SCHEDULE

16. DISTRIBUTION STATEMENT *(of this Report)*

Approved for public release; distribution unlimited.

17. DISTRIBUTION STATEMENT *(of the abstract entered in Block 20, if different from Report)*

18. SUPPLEMENTARY NOTES

19. KEY WORDS *(Continue on reverse side if necessary and identify by block number)*

Warm Fog
Fog Chamber Instrumentation
Electrical Fog Dissipation
Fog Chamber Construction
Warm Fog Dispersal

20. ABSTRACT *(Continue on reverse side if necessary and identify by block number)*

A 27-cubic-foot fog chamber was constructed to investigate fog clearing by electrical means. Fogging of the chamber was accomplished with a spray nozzle driven by pre-humidified air, producing water droplets ranging from 10μ to 75μ. A corona discharge head in the center of the chamber was operated from 0 to 100 kV and measurements of fog conditions were made optically and with coated slides placed at various positions

DD FORM 1 JAN 73 1473 EDITION OF 1 NOV 65 IS OBSOLETE
S/N 0102-014-6601 |
(Page 1)

UNCLASSIFIED

SECURITY CLASSIFICATION OF THIS PAGE *(When Data Entered)*

in the chamber. Rapid clearing was caused by the corona discharge. The dominant clearing mechanisms identified were coalescence and pushing of charged droplets to the walls of the chamber; the small size of the chamber precluded determination of which mechanism would be most important in large-scale fog clearing.

Thesis
H494
c.1

147959

Herman
Laboratory investigation of electrical dissipation of warm fog.